November 2000 • NREL/SR-520-29227

Subcontractor Report

Process Development for CIGS-Based Thin-Film Photovoltaic Modules

Phase II Technical Report

J. Britt, S. Wiedeman, and S. Albright
Global Solar Energy, L.L.C.
Tucson, Arizona

National Renewable Energy Laboratory

1617 Cole Boulevard
Golden, Colorado 80401-3393

NREL is a U.S. Department of Energy Laboratory
Operated by Midwest Research Institute • Battelle • Bechtel

Contract No. DE-AC36-99-GO10337

November 2000 • NREL/SR-520-29227

Process Development for CIGS-Based Thin-Film Photovoltaic Modules

Phase II Technical Report

J. Britt, S. Wiedeman, and S. Albright
Global Solar Energy, L.L.C.
Tucson, Arizona

NREL Technical Monitor: H.S. Ullal

Prepared under Subcontract No. ZAK-8-17619-04

National Renewable Energy Laboratory

1617 Cole Boulevard
Golden, Colorado 80401-3393

NREL is a U.S. Department of Energy Laboratory
Operated by Midwest Research Institute • Battelle • Bechtel

Contract No. DE-AC36-99-GO10337

NOTICE

Available electronically at http://www.doe.gov/bridge

Available for a processing fee to U.S. Department of Energy
and its contractors, in paper, from:

U.S. Department of Energy
Office of Scientific and Technical Information
P.O. Box 62
Oak Ridge, TN 37831-0062
phone: 865.576.8401
fax: 865.576.5728
email: reports@adonis.osti.gov

Available for sale to the public, in paper, from:

U.S. Department of Commerce
National Technical Information Service
5285 Port Royal Road
Springfield, VA 22161
phone: 800.553.6847
fax: 703.605.6900
email: orders@ntis.fedworld.gov
online ordering: http://www.ntis.gov/ordering.htm

Printed on paper containing at least 50% wastepaper, including 20% postconsumer waste

Table of Contents

List of Figures

List of Tables

Abstract

As a technology partner with NREL, Global Solar Energy (GSE) has initiated an extensive and systematic plan to accelerate the commercialization of thin film photovoltaics (PV) based on Copper Indium Gallium Diselenide (CIGS). The distinguishing feature of the GSE manufacturing process is the exclusive use of lightweight, flexible substrates. GSE has developed the technology to fabricate CIGS photovoltaics on both stainless steel and polymer substrates. CIGS deposited on flexible substrates can be fabricated into either flexible or rigid modules. Low-cost, rigid PV panels for remote power, bulk/utility, telecommunication, and rooftop applications have been produced by affixing the flexible substrate to an inexpensive rigid panel by lamination or adhesive.

In the GSE approach, continuous rolls of substrate as long as 1000 feet are processed as opposed to individual small glass plates. Stainless steel based PV modules are fabricated by a novel interconnect method that avoids the use of wires or foils and soldered connections. In the case of polymer based PV modules, the continuous roll is not sectioned into individual panels until the module buss and power leads are attached. Roll-to-roll vacuum deposition has several advantages that translate directly to reduced capital costs, greater productivity, improved yield, greater reliability, lower maintenance, and a larger volume of PV material.

In combination with roll-to-roll processing, GSE has developed evaporation deposition operations that enable low-cost and high-efficiency CIGS modules. In-line multi-source evaporation has been demonstrated at GSE to deposit high-quality CIGS films in a continuous roll-to-roll operation. Multi-source evaporation has other advantages including direct absorber formation (no selenization heat treatment) and high materials utilization of low-cost feed stock.

The CIGS deposition process relies heavily on effusion source technology developed at GSE, and solving numerous problems was an integral part of the source development effort. At present, the robust effusion sources are capable of depositing high-quality coatings over large areas. Significant challenges still exist for increasing the source capacity to enable even longer depositions and improving the control of effusion rate during production runs.

CIGS process development is focused on synchronizing the operation of the effusion sources, delivery profile, substrate temperature, and a host of other parameters. The primary vehicle for CIGS process development was shifted from a 6.5-inch R&D web coater to a 12-inch pilot production system in Phase II. In addition, a program initiated in Phase I to introduce a stainless steel foil based product as a complement to polyimide was expanded in Phase II resulting in a GSE record cell efficiency of 11.5% (NREL verified) on stainless steel. A 19.7W prototype module product based on stainless steel with an aperture area efficiency of 7.3% was demonstrated.

Cell interconnection for thin film CIGS modules on a polyimide substrate presents a considerable challenge. Substantial progress has been made in the development of all-laser processes for monolithic integration. The interconnect scheme requires both an ink-jet deposition step and the removal of material by selective laser scribing. All laser scribes have been demonstrated and optimized to minimize electrical losses. Continuous ink-jet lines less than 200μm in width are routinely achieved, a noticeable advantage over screen-printing.

In the area of new product development and demonstration progress has been made in several fields. Unlaminated submodules on a rigid substrate for use as roof top shingles have been developed with a strategic business partner. Modules utilizing a reinforced nylon backing are the basis for two GSE product lines with attributes of lightweight, durability, and portability. Modules that utilize a semi-rigid, thin aluminum backing for added strength in the field and for a standard UL rate-able product line have been demonstrated. The semi-rigid module designs have been submitted to UL and a contract for UL testing is in place. Critical product certification equipment has been procured and validated at the GSE Tucson facility to accelerate the required testing. Products have been demonstrated in selected market sectors for early feedback from customers.

INTRODUCTION

Thin film photovoltaic (PV) modules are the next evolutionary step towards cost-effective generation of electricity from sunlight. Thin film Copper Indium Gallium (CIGS) has been established as a leading contender to achieve that goal. Global Solar Energy (GSE) was founded to capitalize on the natural advantages of CIGS and develop a cost-efficient manufacturing scheme to bring the technology to market in a user-friendly form. The heart of the manufacturing scheme is all roll-to-roll vacuum processing on a continuous flexible polyimide substrate.

There are numerous challenges in developing the technology for manufacturing flexible CIGS photovoltaic modules. Three major areas deemed exceptionally challenging were selected by GSE for focused development under the Thin Film Partnership Program: 1) CIGS absorber improvement, 2) monolithic integration, and 3) encapsulation. The deposition of CIGS films on a continuous web by multi-source evaporation had never been attempted by any group before GSE undertook it and many unique difficulties must be confronted. Most conventional techniques for monolithic integration of thin film PV devices on glass substrates cannot be applied to integrate devices on a polyimide substrate. Novel interconnect schemes and processes must be developed. The encapsulation of a flexible module also presents special problems to solve, and unique advantages to employ.

The primary issues that are being addressed to improve the CIGS absorber are control of the effusion sources and development of processes that yield high-quality CIGS thin films. In particular, scaling up the source design for multi-source coevaporation over large areas (33-cm × 300-meter rolls of substrate) with adequate uniformity is an important goal. Significant improvements to the effusion source design and operation were made in Phase II. At present, the robust effusion sources are capable of depositing high quality coatings over large areas. Significant challenges still exist for increasing the source capacity to enable even longer depositions and improving the control of effusion rate during production runs.

Another significant accomplishment that occurred during Phase II was the demonstration of a 11.5% device from CIGS deposited on stainless steel web. That milestone was the result of a deeper understanding of the CIGS deposition process as practiced by GSE. In addition, process improvement tests validated the beneficial effects of Na doping which was subsequently implemented in the production equipment. The compatibility of GSE processes for CdS and the TCO depositions was continuously verified as improvements in the absorber deposition process were made.

Substantial improvement of the monolithic integration of PV cells on polyimide substrate has been made. Most aspects of the back contact, via, and front contact scribes have been rigorously verified by electrical and microscopic techniques. The ink dispense technology, an integral part of the interconnect scheme, has demonstrated continuous ink lines less than 200 μm wide, with exceptional reproducibility.

Numerous accomplishments within the new product development and demonstration area at GSE have been achieved. Unlaminated submodules on a rigid substrate for use as a shingle on the

roofs of houses have been developed with a strategic business partner. Modules that utilize a reinforced nylon backing that provide support for two GSE product lines with attributes of lightweight, durability, and portability have also been developed. Modules that utilize a semi-rigid, thin aluminum backing for added strength in the field and for a standard UL rate-able product line have been demonstrated. The semi-rigid module designs have been submitted to UL and a contract for UL testing is in place. Critical product certification equipment has been procured and validated at the GSE Tucson facility to accelerate the required testing. Products have been demonstrated in selected market sectors for early feedback from customers.

1.0 CIGS ABSORBER IMPROVEMENT

GSE has demonstrated a manufacturable roll-to-roll process for CIGS deposition on a 16.5-cm wide substrate by multi-source evaporation using an efficient source design. The overall objectives of this task are to improve the electronic quality of the absorber material and to refine and scale up the source design for multi-source evaporation over large area (33-cm × 300-m rolls of substrate) with adequate uniformity. Control and reproducibility are critical issues continually addressed in the course of this work.

1.1 Deposition Process Optimization

Deposition parameters are adjusted for the CIGS layer to obtain improved electronic material quality. A 6-inch roll coater is employed as a test platform for the CIGS deposition process. Improvements made to the deposition process in the 6-in roll coater are translated and implemented in the manufacturing system. The manufacturing system utilizes a 13-inch wide web and differs from the 6-inch roll coater primarily in the sophistication of its components. Deposition parameters that are studied include substrate temperature profile, selenium delivery profile, coating thickness, and final elemental composition.

An investigation of stainless steel web initiated in Phase I continued into Phase II. Stainless steel allows much higher substrate temperatures than polyimide, which has a maximum working temperature of 450°C. This should present a considerable advantage in regards to CIGS material and device properties based on the fact that world record efficiency CIGS devices have been deposited at a substrate temperature near 550°C. For the purposes of technical reporting, the two web materials are considered independently.

A series on experiments was initiated to determine the optimum substrate deposition temperature for stainless steel in the 6-inch coater. Three CIGS depositions were conducted at substrate temperatures of 500°, 550°, and 600°C. As it is not practical to monitor the web temperature directly, the temperature is estimated with a thermocouple located adjacent to the center of the web, between the substrate heaters and the web. All the films were doped with ostensibly identical amounts of Na. The films were characterized by Energy Dispersive X-ray spectroscopy (EDX), Scanning Electron Microscopy (SEM), and Auger Electron Spectroscopy (AES) depth profiling at NREL.

The apparent grain size was observed to increase with substrate temperature (Fig. 1.1). Although little or no difference is observed in the profiles of Cu/(Ga+In) (Fig. 1.2), the films show an increasing homogenization of Ga/(Ga+In) with an increase in substrate temperature (Fig. 1.3). The composition Cu/(Ga+In) of these same films by EDX (20kV) indicated that they were Cu-poor. The indication by AES that the films were Cu-rich is likely due to miscalibration.

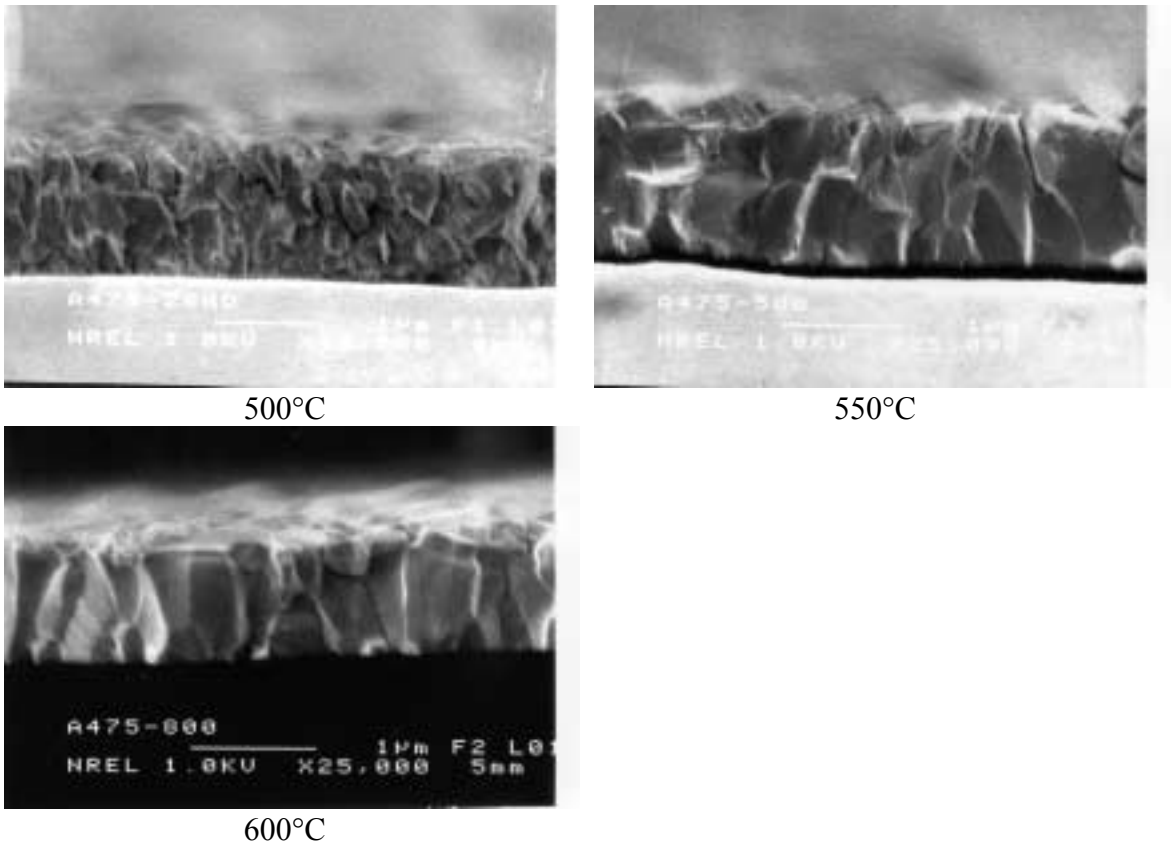

Figure 1. 1 SEM cross-sections of CIGS films deposited at 500°, 550°, and 600°C

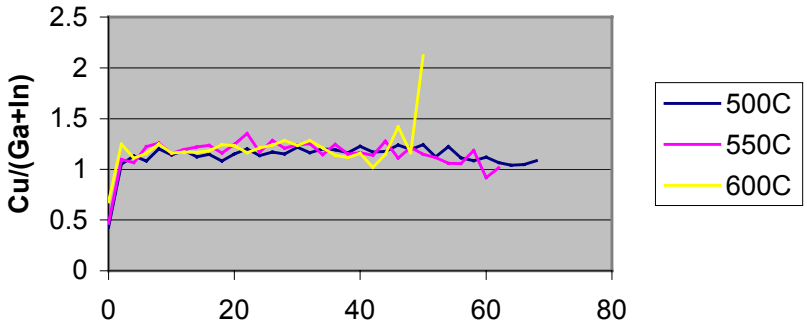

Figure 1. 2. Cu/(Ga+In) for films deposited at 500°, 550°, and 600°C.

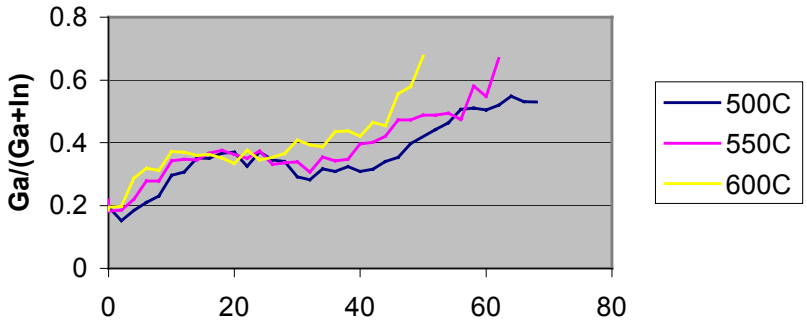

Figure 1. 3 Ga/(Ga+In) for films deposited at 500°, 550°, and 600°C.

SS/Mo/CIGS samples were also extracted from each deposition and fabricated into devices at NREL. The J-V results are summarized in Table 1.1. A clear trend of increasing efficiency with increasing substrate temperature was observed, consistent with the increase in apparent grain size and the Ga profile.

Table 1. 1 JV characteristics of CIGS films deposited at 500°, 550°, and 600°C.

sample	T_{sub} (°C)	V_{oc} (mV)	J_{sc} (mA/cm^2)	FF (%)	Eff. (%)	R_s	R_{sh}
A475-26NO	500	559	26.1	55.7	8.14	3.7	205
A475-50O	550	519	27.1	63.4	8.93	2.4	87
A475-80O	600	532	28.8	64.9	9.93	2.3	210

After it was determined that the optimum substrate temperature for CIGS deposition on stainless steel was substantially higher than what was being used for deposition on polyimide, a set of experiments was conducted to optimize the Se flux. Reaction kinetics are faster at higher substrate temperatures and less Se may be required. CIGS films were deposited on stainless steel web at a nominal substrate temperature of 600°C, using Se source temperatures of 390°, 410°, and 430°C. In this temperature range, the equilibrium vapor pressure approximately doubles every additional 20°C. A Se source temperature of 390°C is typically used for deposition on polyimide films. Again, all the films were doped with ostensibly identical amounts of Na.

The films were characterized by EDX, SEM, and AES depth profiling at NREL. The apparent grain size was observed to increase with Se source temperature (Fig. 1.4). The composition Cu/(Ga+In) of the films by EDX (20kV) indicated that they were all Cu-poor. As indicated before, the indication by AES that the films were Cu-rich is likely due to miscalibration. Slight differences were observed in Cu/(Ga+In) near the film surfaces (Fig. 1.5). The film deposited with the highest Se source temperature (430°C) is significantly less Cu-poor near the film surface than the films that were deposited using lower Se source temperatures. No significant difference in Ga/(Ga+In) was observed between the three films (Fig. 1.6).

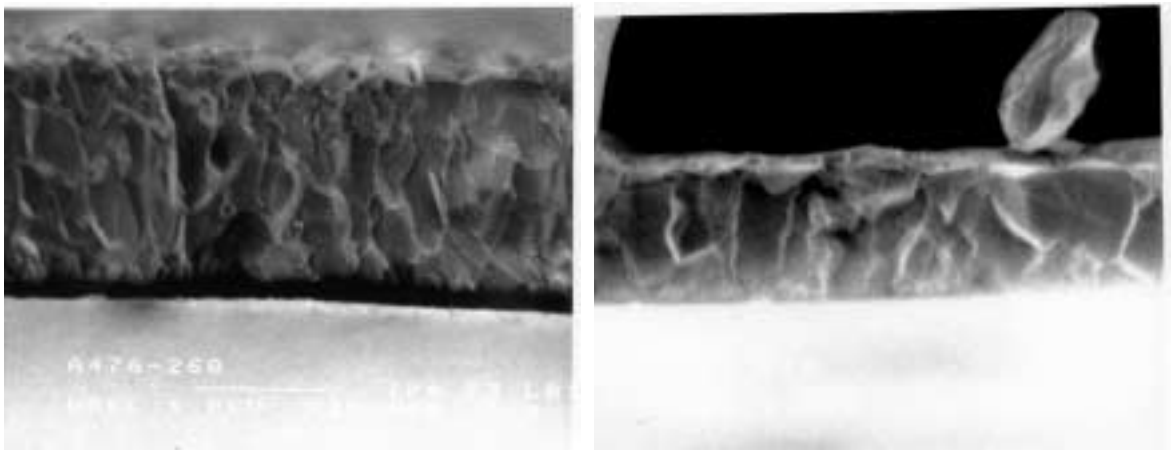

T_{Se}=390°C T_{Se}=410°C

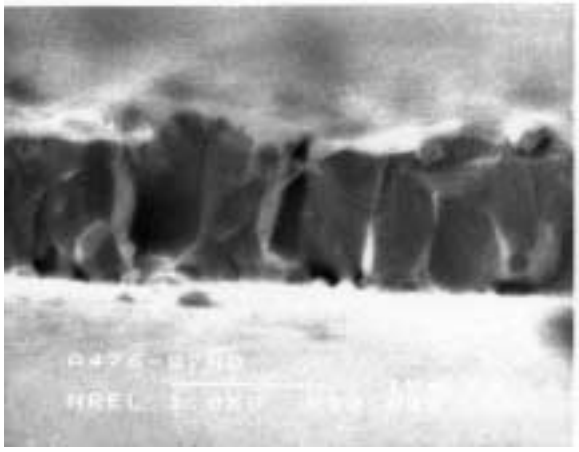

T_{Se}=430°C

Figure 1. 4 SEM cross-sections of CIGS films deposited using Se source temperatures of 390°, 410°, and 430°C

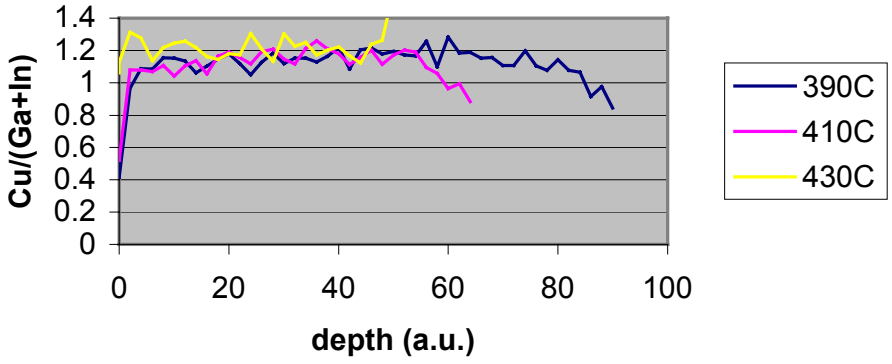

Figure 1. 5 Cu/(Ga+In) of CIGS films deposited using Se source temperatures of 390°, 410°, and 430°C.

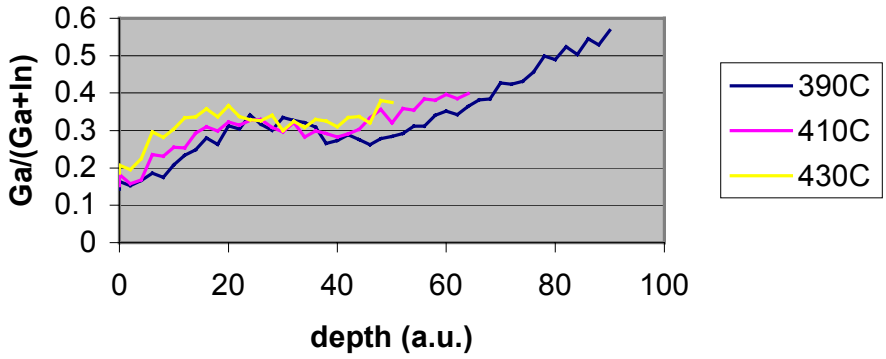

Figure 1. 6 Ga/(Ga+In) of CIGS films deposited using Se source temperatures of 390°, 410°, and 430°C.

CIGS coated SS/Mo samples were also extracted from each deposition and completed into devices at NREL. The J-V results are summarized in Table 1.2. A clear trend of increasing efficiency with increasing Se source temperature was observed. Series and shunt resistance (R_s and R_{sh}, res.) improved with increased Se source temperature.

Table 1. 2 JV characteristics of CIGS films deposited at Se source temperatures of 390°, 410°, and 430°C.

sample	T_{se} (°C)	V_{oc} (mV)	J_{sc} (mA/cm^2)	FF (%)	Eff. (%)	R_s	R_{sh}
A476-26O	390	473	20.6	47.5	4.61	6.3	205
A476-62O	410	560	27.6	58.6	9.05	4.3	538
A476-87NO	430	547	29.2	62.0	9.89	3.4	2150

Based on encouraging results achieved in the 6-inch web coater, a series of trial CIGS depositions were conducted early in Phase II on stainless steel web in the production-based system capable of processing 13-inch wide by up to 1000-foot long rolls. In the trials, CIGS was deposited on approximately twenty 50-foot long stainless steel web sections. The majority of the CIGS-coated webs were processed through all deposition steps in order to fabricate devices.

Several changes were made to the deposition chamber during the course of these trials, generally to adapt the production-based system to process stainless steel. For instance, the substrate heater assembly was modified to reach higher temperatures while remaining robust in the corrosive Se vacuum environment**.** The higher temperatures necessary to take advantage of the properties of stainless steel led to a substantially hotter chamber and subsequent increase in processing pressure. Accordingly an additional high-vacuum pump was added to double system pumping capability. An effusion source for a sodium precursor was also installed in the 13-inch system based on the outcome of experiments conducted in the 6-inch web coater (see Section 1.3).

After these trials, the 13-inch production-based CIGS roll-to-roll coater was modified to allow the deposition of CIGS films via the three-stage technique based upon the experiences of GSE team members and the world record efficiencies obtained at NREL. After modifying the equipment configuration and calibrating the temperature profile through the deposition zones, a set of CIGS calibration runs were conducted. The initial results after the reconfiguration were not encouraging; efficiencies were low due to poor short-circuit currents (8-15 mA/cm^2) and fill factors (25-45%). In addition, the film morphology was poor with very small grains.

Subsequently, a series of process improvement tests were conducted that led to improved morphology. A corresponding improvement in J_{sc} and FF was correlated to the improved morphology. The following series of pilot production runs were substantially improved, with long sections of web having sample device efficiencies in the 7-9% range. Process refinement continued from this point, focusing on in-process profiles of Cu/(Ga+In) and Se flux.

1.2 Source Scale-Up

Effusion sources for multi-source evaporation must be mechanically and electrically robust and allow tight flux rate control and spatial uniformity across the substrate width. In addition, the sources must be very efficient to eliminate heat load on the substrate and system parts. Scaled-up effusion sources for deposition on 33-cm substrate widths (for roll coating 33-cm × 300-meter of substrate) have been designed, fabricated, tested, and implemented based on existing proven designs used in the 15-cm roll-coater. Effusion profile and rate modeling done in collaboration with the Institute of Energy Conversion (IEC), University of Delaware as a subcontractor have aided this effort.

Careful design and selection of materials are necessary for constructing well-behaved effusion sources. The Cu source in particular demands great attention to detail as it is required to operate at temperatures greater than 1500°C in the presence of Se for long periods of time. The list of materials capable of sustained functioning in this environment is short. Successful source designs must account for thermal conductivity and expansion of all critical parts.

Many improvements in the design and operation of the effusion sources have been made during Phase II. Heater element failure was virtually eliminated by improving the installation procedure. Deposition material build-up was substantially lessened with better design and operation. The heat load to the web was adjusted by optimizing the insulation surrounding the effusion source. Excessive insulation was not applied, as some waste heat is desirable for heating the web.

1.3 Efficiency Improvement Studies

The effusion model developed at IEC for the GSE CIGS deposition systems was used extensively during Phase II. The accuracy of the model allowed prediction of the extent to which the CIGS films could be driven into the Cu-rich regime during the deposition process. The capability allowed more precise experiments to be performed to quantify the effect of composition excursions on material properties and device performance. Since the substrate temperatures employed are substantially different, experiments were performed on both polyimide and stainless steel web to identify any substrate temperature related differences.

Figure 1.7 shows the surface morphologies of two CIGS films deposited on stainless steel at a nominal substrate temperature of 600°C. The apparent grain size of the film that went through a Cu-rich stage (A) is substantially larger than that of the film that remained Cu-poor during the entire film growth (B), even though the final compositions are nearly identical (by Electron Probe Micro Analysis (EPMA) (20kV), Cu/(Ga+In) = 0.89 and 0.91, respectively). This result is consistent with the accepted theory that Cu_xSe is a fluxing agent that promotes recrystallization at temperatures above its melting point (523°C).

AES depth profile analysis was also performed on the above two films. The results are shown in Figs. 1.8 and 1.9. Surprisingly, the film that remained Cu-poor during the entire film growth (B) is non-uniform in Cu/(Ga+In) through the film thickness. The diffusivity of Cu under these conditions is expected to more than adequate to achieve a uniform through thickness profile. A number of basic assumptions about the process parameters, including substrate temperature, were questioned in light of this result. A satisfactory conclusion could not be arrived at. Under certain conditions, however, it appears that the Cu-rich phase promotes diffusion.

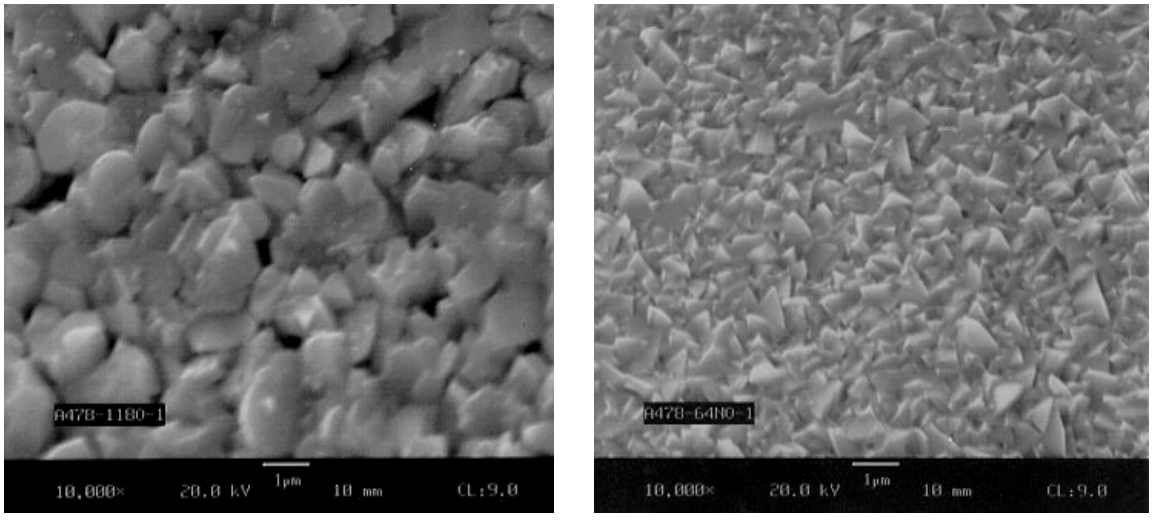

A **B**

Figure 1. 7. Surface morphology of CIGS films deposited on stainless steel with (A) and without a Cu-rich stage (B).

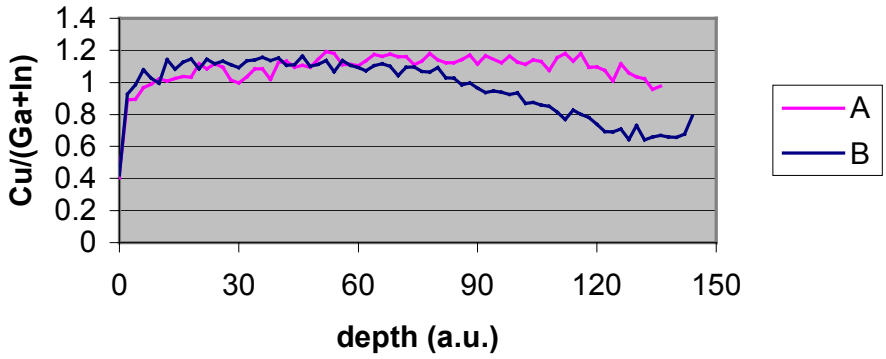

Figure 1. 8 Cu/(Ga+In) of CIGS films deposited on stainless steel with (A) and without a Cu-rich stage (B).

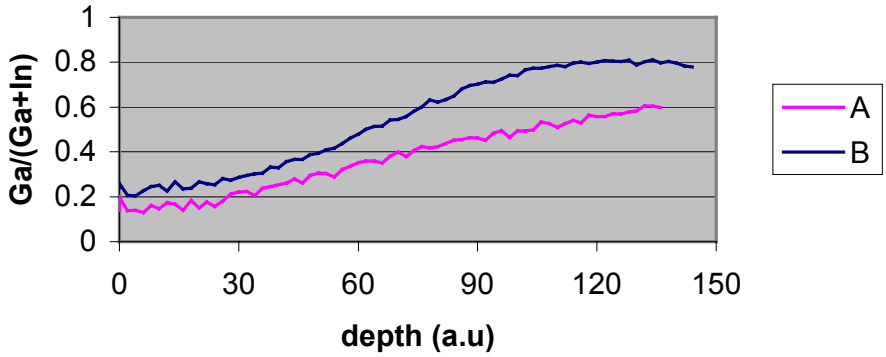

Figure 1. 9 Ga/(Ga+In) of CIGS films deposited on stainless steel with (A) and without a Cu-rich stage (B).

These experiments were repeated on polyimide web at a far lower substrate temperature of 450°C. As before, the apparent grain size of the film that experienced a Cu-rich stage (A) is larger than that of the film that did not (B) (Fig. 1.10). By EPMA, the ratio of Cu/(Ga+In) of films A and B are 0.87 and 0.94, res. The apparent grain size of CIGS deposited on polyimide is substantially smaller than that deposited on stainless steel, probably because of the difference in substrate temperature and lack of liquid phase-assisted grain growth.

As was the case for CIGS films deposited on stainless steel at a higher temperature, the composition depth profile of film B as determined by AES analysis indicates a lack of Cu homogenization (Fig. 1.11). There is also significantly less mixing of Ga and In in CIGS films deposited on polyimide than in the films deposited on stainless steel web. This is reflected in the structured Ga/(Ga+In) profiles (Fig. 1.12) that result from the source ordering. The structure is not apparent in Auger measurements of CIGS films deposited on stainless steel (Fig. 1.9), even though the source ordering is identical. Enhanced diffusion at higher substrate temperature is believed to explain these results.

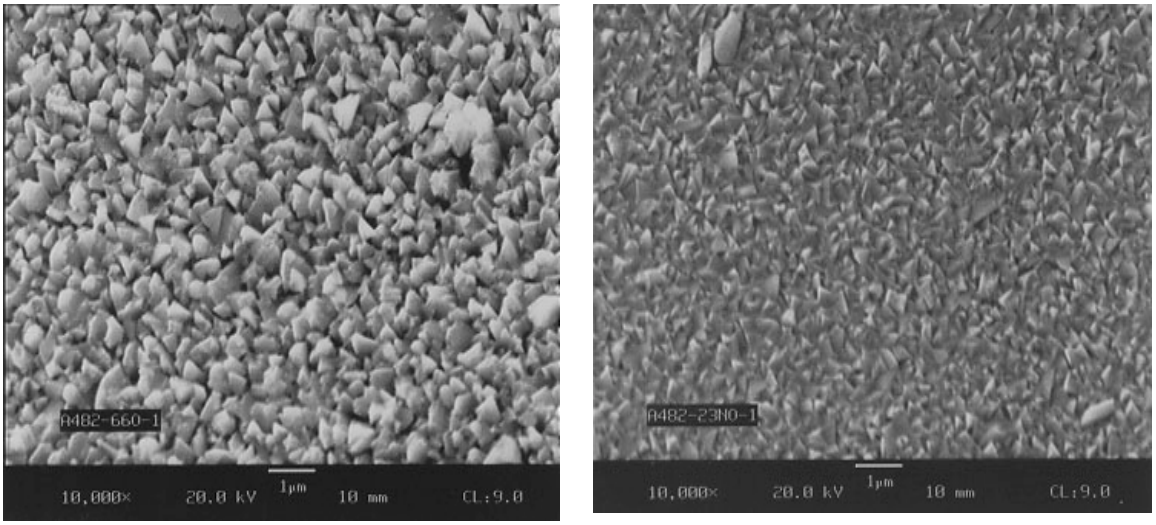

Figure 1. 10 Surface morphology of CIGS films deposited on polyimide with (A) and without a Cu-rich stage (B).

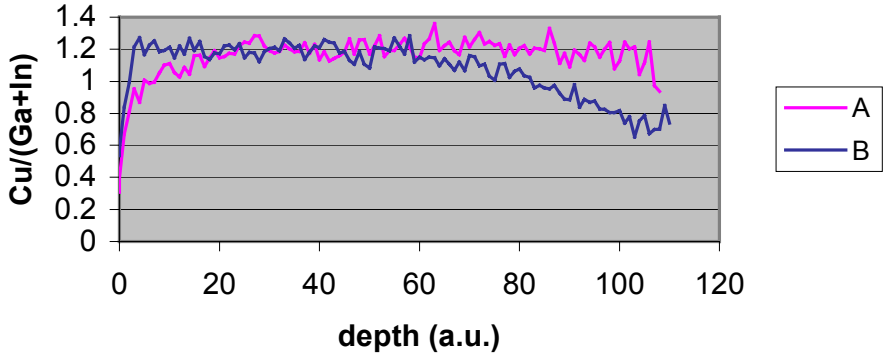

Figure 1. 11 Cu/(Ga+In) of CIGS films deposited on polyimide with (A) and without a Cu-rich stage (B).

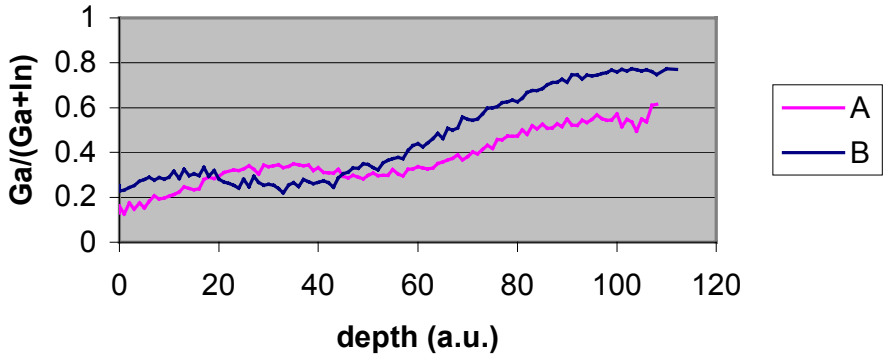

Figure 1. 12 Ga/(Ga+In) of CIGS films deposited on polyimide with (A) and without a Cu-rich stage (B).

The CIGS films deposited on stainless steel and polyimide with and without a Cu-rich growth stage were fabricated into devices at IEC by depositing Chemical Bath Deposition (CBD) CdS, i-

ZnO, and c-ZnO. The devices were characterized by J-V (Tables 1.3 and 1.4) and QE measurements (Figs. 1.13 and 1.14).

With regard to the devices on stainless steel, the CIGS film deposited with a Cu-rich growth stage (A) led to a substantially better fill factor and short circuit current density and efficiency than the CIGS film without such a growth stage (B). A comparison of the quantum efficiencies of these two devices reveals that the difference in J_{sc} is partially due to better IR response in film A. The difference is likely the result of the larger bandgap or smaller grain size of film B.

Table 1. 3 JV characteristics of CIGS devices deposited on stainless steel substrate with and without a Cu-rich stage during CIGS deposition.

sample #	Cu-rich stage	Eff.	FF	V_{oc}	J_{sc}	R_{oc}	G_{sc}
		(%)	(%)	(volts)	(mA/cm^2)	(Ω-cm^2)	(mS/cm^2)
A478-118O-3	yes	11.0	64.4	0.497	34.5	2.0	1.5
A478-64NO-2	no	9.4	59.0	0.522	30.4	2.8	1.6

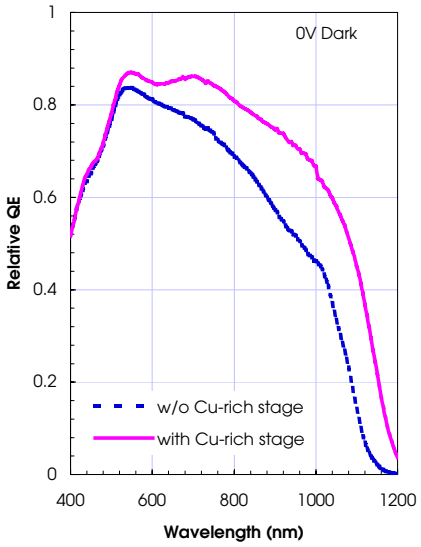

Figure 1. 13 Quantum efficiencies of CIGS devices deposited on stainless steel substrate with and without a Cu-rich stage during CIGS deposition

The device results on polyimide follow the same efficiency trends as on stainless steel, but are more dramatic. The efficiency of the film without a Cu-rich growth stage (B) is half that of the film with a Cu-rich growth stage (A) (Table 1.4). The difference in efficiency is almost entirely due to short circuit current density and fill factor. As before, the QE data shows very poor IR response in film B, but the difference is much more pronounced than was the case for stainless steel (Fig. 1.14). Once again, the larger band gap of film B should result in a somewhat poorer IR response, but such a substantial difference probably implies a substantial recombination loss in film B.

Table 1. 4 JV characteristics of CIGS devices deposited on polyimide substrate with and without a Cu-rich stage during CIGS deposition.

sample #	Cu-rich stage	Eff.	FF	V_{oc}	J_{sc}	R_{oc}	G_{sc}
		(%)	(%)	(volts)	(mA/cm^2)	(Ω-cm^2)	(mS/cm^2)
A482-66O-2	yes	7.90	53.8	0.466	31.5	3.9	3.1
A482-23NO-2	no	3.99	40.9	0.445	22.0	7.4	12.2

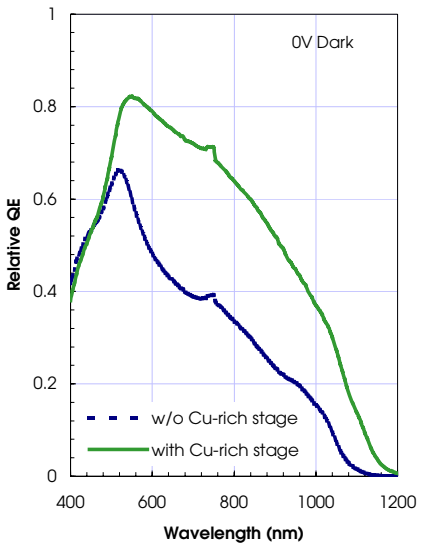

Figure 1. 14 Quantum efficiencies of CIGS devices deposited on polyimide substrate with and without a Cu-rich stage during CIGS deposition.

Impurities and defect introduction are naturally a concern when introducing a relatively novel substrate such as stainless steel into the manufacturing process. Stainless steel rolls are produced by a mechanical process that imparts a surface finish that ranges from matte to mirror-like. In addition, all stainless steels contain Fe, C, and Cr and additional elements added to enhance mechanical, electrical and corrosion properties. Depending on the electronic effect induced in CIGS by a particular impurity, the type of steel used as a substrate for deposition may have a dramatic impact on efficiency. During Phase II, an effort to identify impurities and defects in the CIGS coating that originate in the stainless steel web was initiated.

As an example, CIGS films deposited at 500°, 550° and 600°C on stainless steel were analyzed by SIMS depth profiling (A. Rockett, U. of Ill.) for elements present in steel. Higher temperatures are expected to promote the diffusion of impurities into the CIGS coating. The results are shown in Fig. 1.15 for the elements Fe, Cr, and C. The signals are normalized to the Se signal. The signals for all three elements were found to be very low in the CIGS films and rise when sampling into the steel itself. This is expected as the Se signal drops there. No clear trend was observed with substrate temperature. The latter observation may imply that impurity diffusion for these elements is not a serious concern.

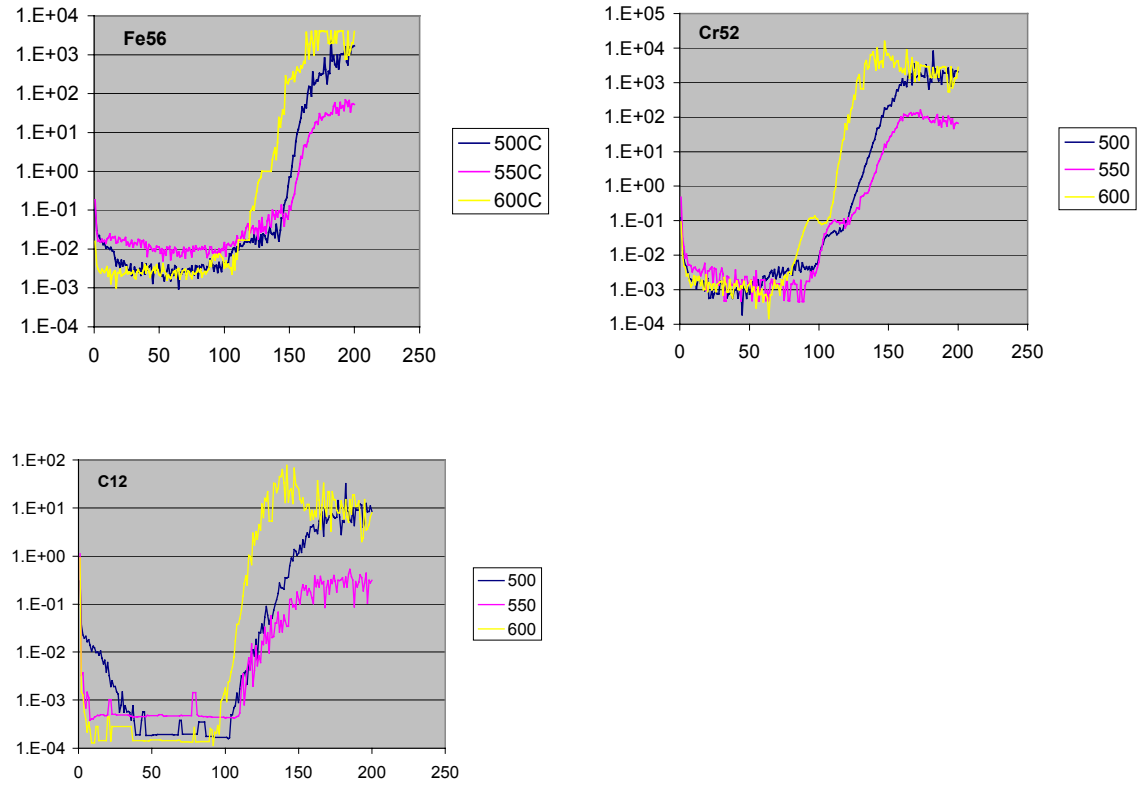

Figure 1. 15 SIMS depth profiles for the elements Fe, Cr, and C in CIGS films deposited on stainless steel at substrate temperatures of 500°, 550° and 600°C.

Additional work has been done to identify the physical defects observed on stainless steel webs and the CIGS films deposited on them. As a part of continuous quality control, every lot of stainless steel received by GSE is inspected for defects. In many cases, attempts have been made to quantify the effect of such defects on device performance. The analysis of defects and impurities and their impact on yield and peak efficiency will continue in Phase III.

1.3.1 Na Incorporation

Na doping was investigated for both stainless steel and polyimide substrates in the 6-in. reactor. A Na precursor was deposited *in-situ* on the surface of the back contact prior to CIGS deposition for all experiments. Since the deposition uniformity is poor from the effusion source employed, a maximum coating thickness of 200Å was targeted. This value was chosen based on previous results that indicated a loss of adhesion for films thicker than 200Å. The variation of coating thickness across the web width was approximately ± 50%.

The effect of substrate temperature on Na incorporation in CIGS films deposited on stainless steel was investigated. It was hoped that the information gained would indicate the efficacy of Na doping at the lower temperatures required for deposition on polyimide substrate. The experiment was done by ramping the substrate temperature during a single CIGS deposition from

500 to 600°C. Samples were extracted from the web that had CIGS deposited at 500°, 550°, and 600°C, as well as a control sample deposited at 600°C with no Na precursor.

SIMS depth profiling for Na was performed on all four samples. The results are plotted in Fig. 1.16 normalized to the Se signal. All intentionally doped samples showed Na levels an order of magnitude greater than the control sample. There is no clear correlation between substrate temperature and Na level in the intentionally doped samples. This may be attributed to variations in Na precursor thickness or CIGS morphology. The film deposited at 500°C, for instance, has poorer morphology than the films deposited at 550° and 600°C with consequently greater grain boundary area for Na to diffuse into. The only clear conclusion that can be drawn from this data is that the intentionally doped samples have substantially higher Na signals than the control sample.

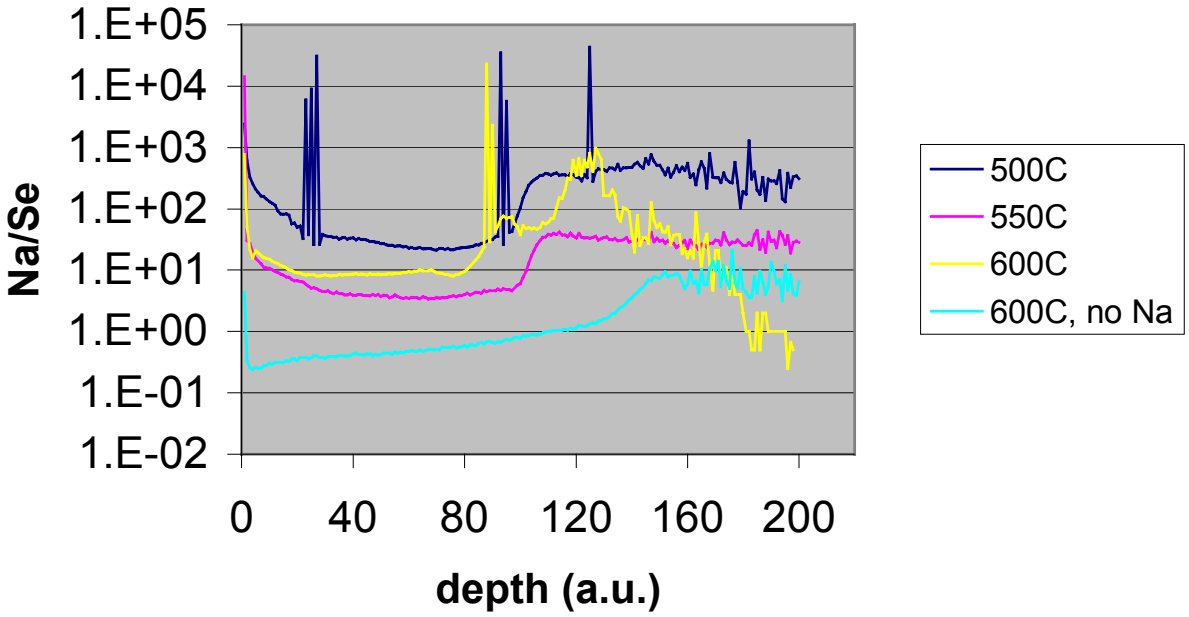

Figure 1. 16 SIMS depth profiles of Na in CIGS films deposited at 500°, 550°, and 600°C.

Repeated observations have correlated Na-doped CIGS films with poorer morphology. This is illustrated in Fig. 1.17 and Fig. 1.18 for CIGS films deposited during a single deposition with and without a Na precursor (on stainless steel and polyimide web, respectively). The Na precursor may interfere with the initial nucleation of the CIGS film.

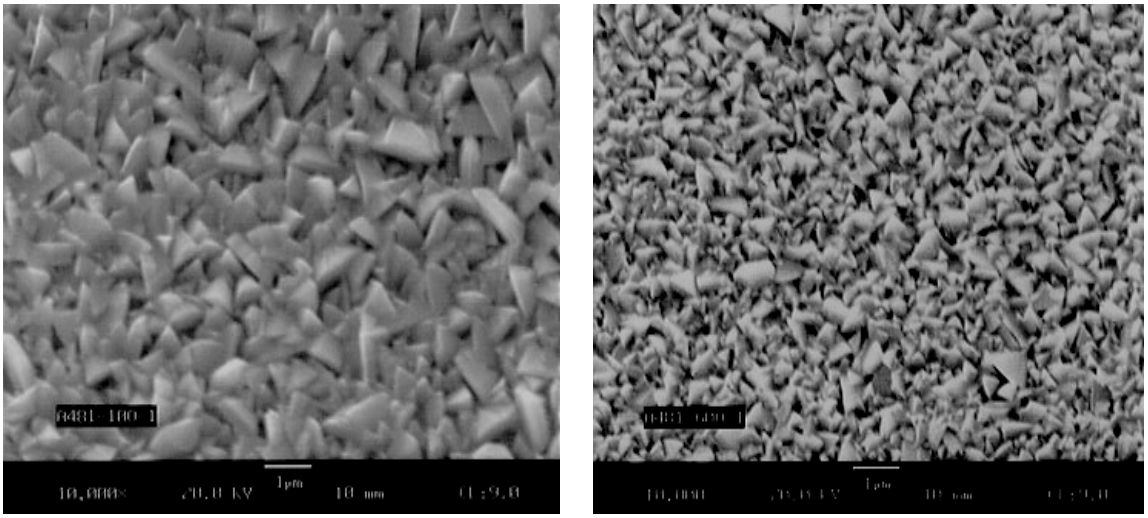

w/o Na doping with Na doping

Figure 1. 17 Surface morphology of CIGS films deposited on stainless steel without and with Na doping.

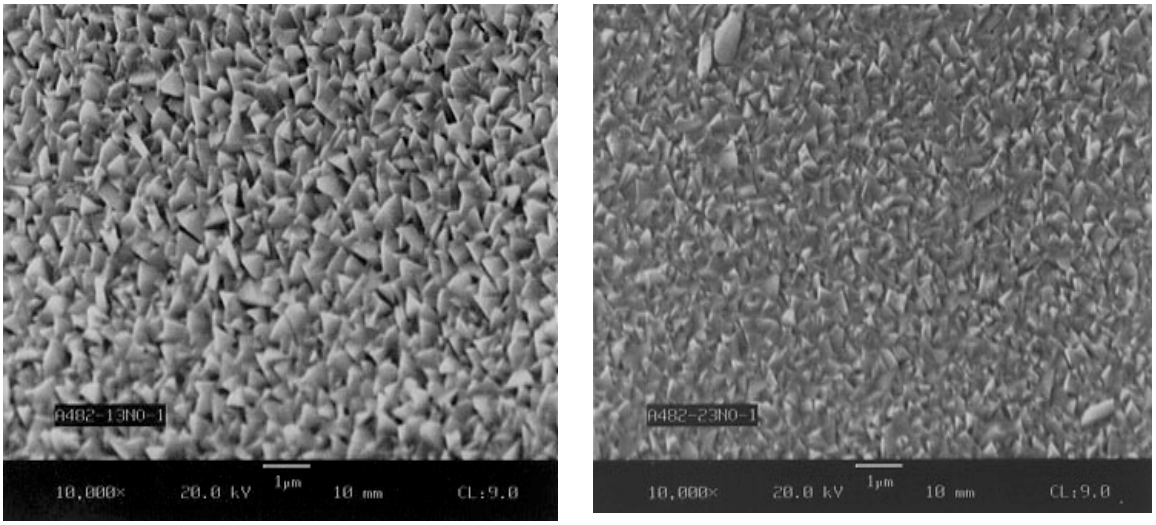

w/o Na doping with Na doping

Figure 1. 18 Surface morphology of CIGS films deposited on polyimide without and with Na doping

Of course, the effectiveness of Na doping is ultimately determined by device efficiency. Uniform improvements in efficiency have been noted on both stainless steel and polyimide based devices upon doping with Na (Tables 1.5, 1.6). Improvements are generally found in all device parameters, but the most significant improvement is observed in V_{oc} and fill factor. The smaller improvement in J_{sc} has been found to be due to a spectrally independent improvement in quantum efficiency (Fig. 1.19).

Table 1. 5 JV characteristics of CIGS devices on stainless steel with and without Na doping.

sample #	Na doped	Eff.	FF	V_{oc}	J_{sc}	R_{oc}	G_{sc}
		(%)	(%)	(volts)	(mA/cm^2)	(Ω-cm^2)	(mS/cm^2)
A481-10O-2	no	5.83	48.3	0.432	28.0	5.4	5.0
A481-60O-2	yes	8.59	55.7	0.542	28.5	3.0	4.3

Table 1. 6 JV characteristics of CIGS devices on polyimide with and without Na doping.

sample	Na doped	Eff.	FF	V_{oc}	J_{sc}	R_{oc}	G_{sc}
		(%)	(%)	(volts)	(mA/cm^2)	(Ω-cm^2)	(mS/cm^2)
A482-114O-2	no	5.05	43.7	0.411	28.2	6.2	10.0
A482-66O-2	yes	7.90	53.8	0.466	31.5	3.9	3.1

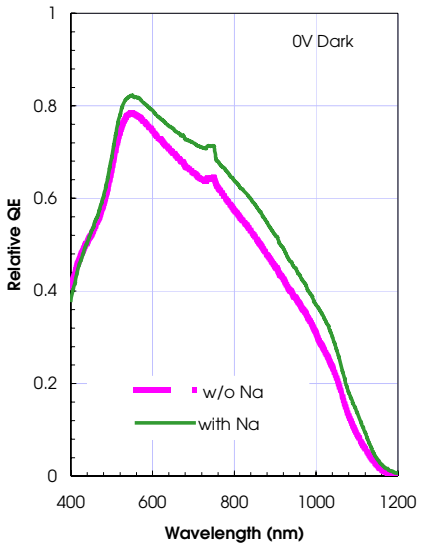

Figure 1. 19 QEs of CIGS devices on polyimide with and without Na doping.

A GSE record efficiency (11.5%, verified at NREL), was fabricated during the Na-doping tests (Fig. 1.20). The CIGS was deposited at GSE on stainless steel web in the 6-in coater. Device fabrication was completed at IEC (CBD CdS, i-ZnO, c-ZnO, grids). The good device result partially stimulated the series of trial depositions in the manufacturing system on stainless steel. Several devices with efficiency greater than 11% were submitted to the contract monitor (H. Ullal) thereby satisfying a major Phase II GSE Thin Film Partnership contract deliverable.

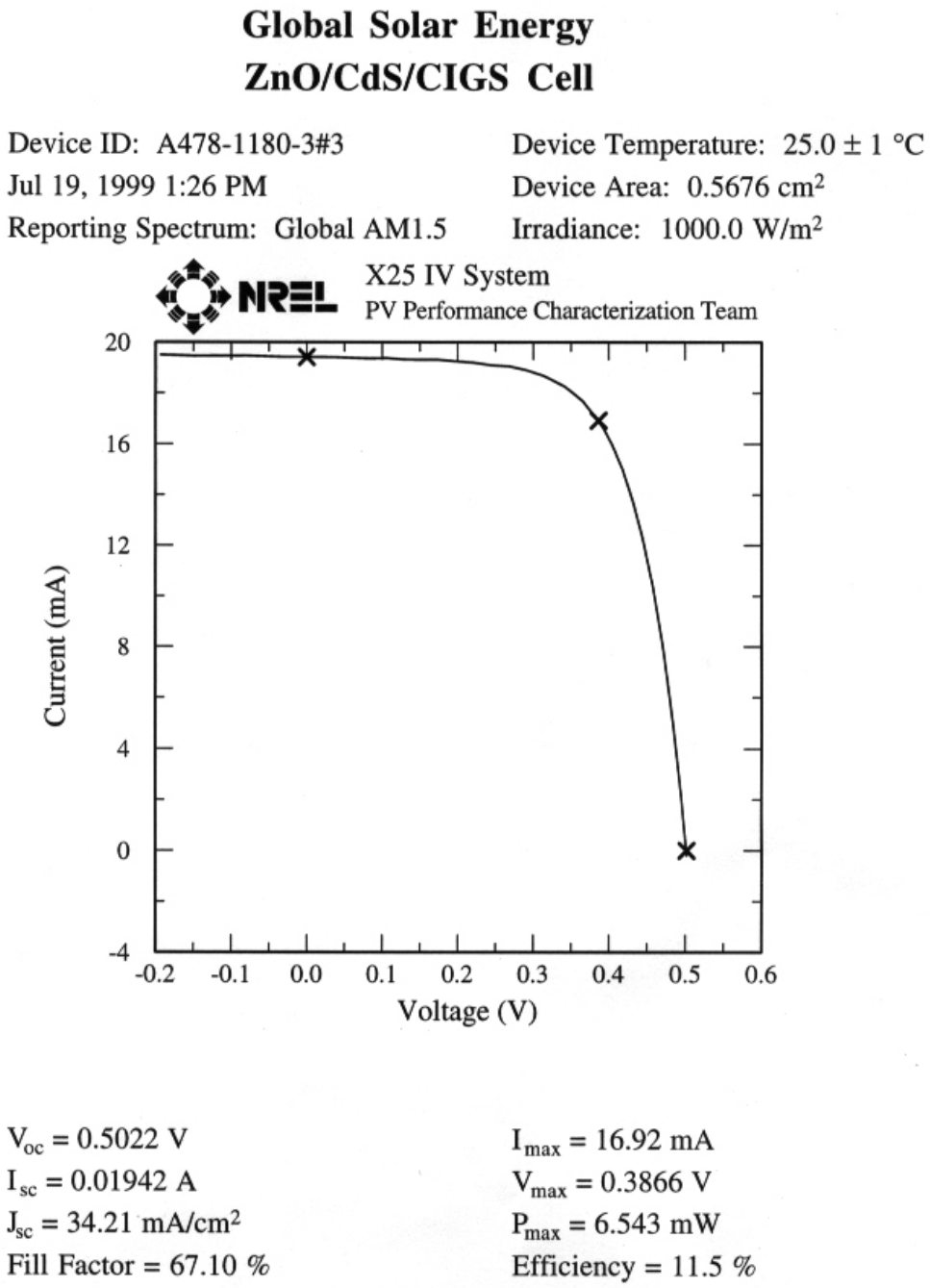

Figure 1. 20 Device characteristics of an 11.5% GSE CIGS device on stainless steel measured at NREL.

The first GSE submodules based on stainless steel were also fabricated and characterized. Several lightweight, foldable modules were assembled from the submodule elements. The IV measurement of the best module is shown in Fig. 1.21. The power output of the module is 19.7W with an aperture efficiency of 7.3%.

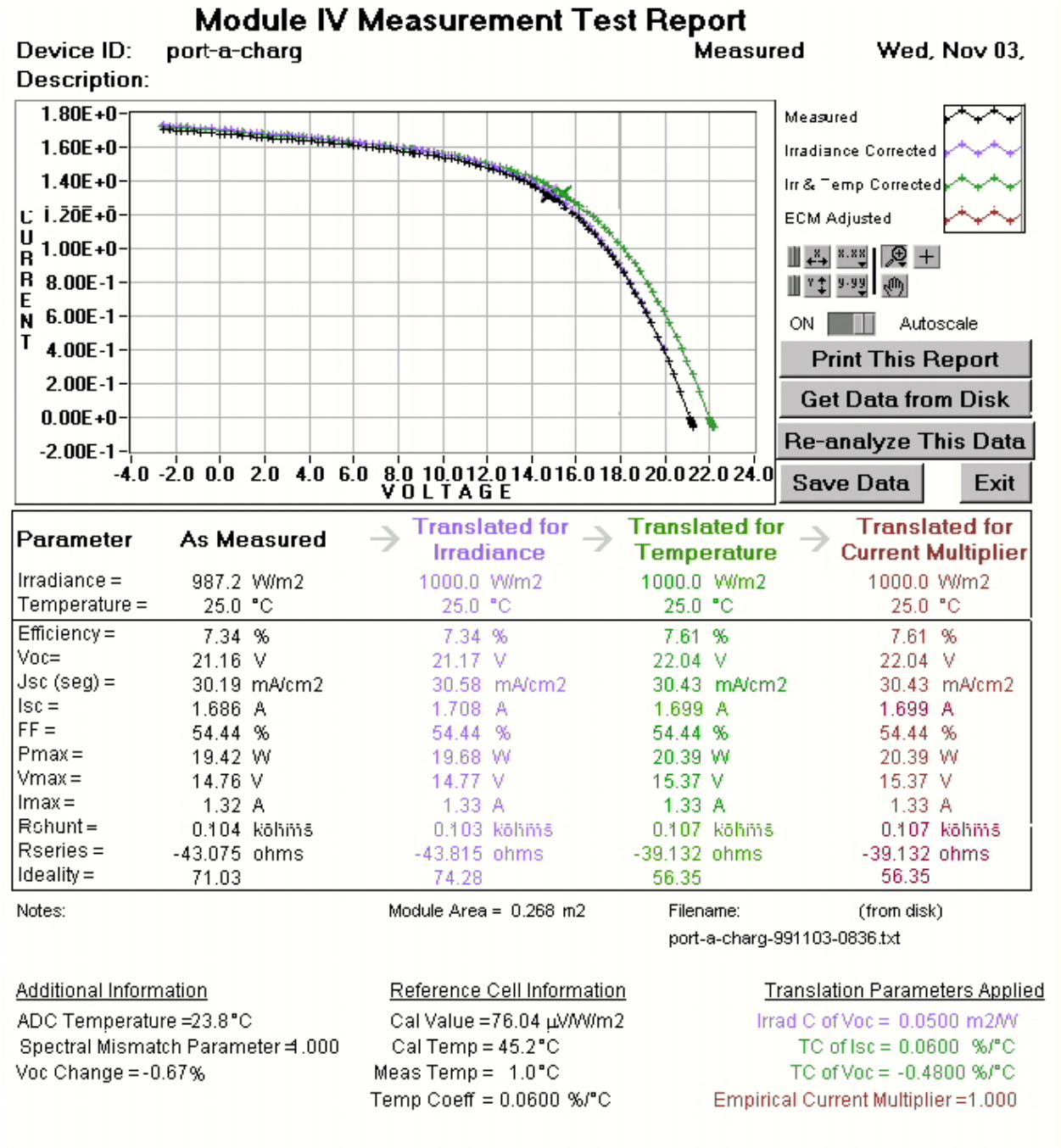

Figure 1. 21 Outdoor JV characteristics of a flexible GSE module on stainless steel.

1.4 Heterojunction Formation Capability

Further comparisons were made during the quarter between the IEC and GSE window layers (CdS and TCO). The IEC window layer consists of chemical bath CdS, sputtered insulating ZnO, and sputtered conducting ZnO. GSE utilizes all-vacuum processing for its window layer coating. Common CIGS deposited on stainless steel at GSE was used for each set.

The JV characteristics for each set are shown in Table 1.7. The four CIGS samples were deposited in two runs under nominally identical conditions. The all-GSE devices are slightly inferior to the ones made at IEC with no clear trend in effect on one parameter over another, with the exception of a smaller short-circuit conductivity (G_{sc}) for the IEC finished devices. The quantum efficiencies of two of these devices with GSE and IEC windows are compared in Figure 1.22. The major difference is the superior blue response of the IEC window. This may be attributed to the different techniques (and thicknesses) by which CdS was deposited.

Table 1. 7 JV characteristics of devices fabricated with IEC and GSE windows.

Sample #	Window	Eff.	FF	V_{oc}	J_{sc}	R_{oc}	G_{sc}
		(%)	(%)	(volts)	(mA/cm^2)	(Ω-cm^2)	(mS/cm^2)
A475-84O-3	IEC	8.89	60.3	0.537	27.5	3.2	1.4
A475-82O-3	GSE-1	8.39	57.2	0.522	28.1	2.7	9.0

Sample #	Window	Eff.	FF	V_{oc}	J_{sc}	R_{oc}	G_{sc}
		(%)	(%)	(volts)	(mA/cm^2)	(Ω-cm^2)	(mS/cm^2)
A476-86O-2	IEC	9.62	62.6	0.525	29.3	2.6	0.7
A476-85O-2	GSE-1	7.86	61.3	0.493	26.0	2.7	4.0

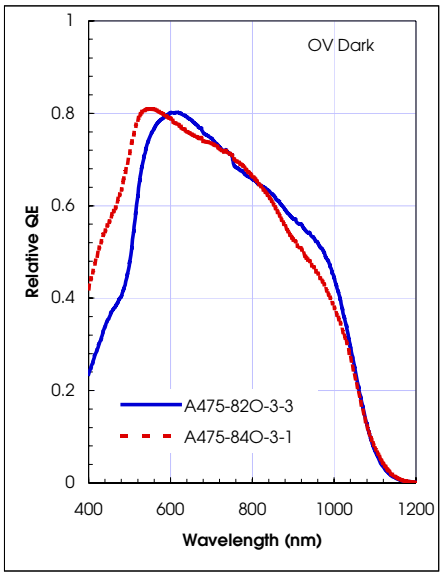

Figure 1. 22 Quantum efficiencies of devices with windows deposited at IEC (A475-84O-3-1) and GSE (A475-82O-3-3).

Later in Phase II, less emphasis was placed on 'laboratory-scale' window processes for finishing and qualifying CIGS films and the focus was shifted towards GSE roll-to-roll processes conducted in production-based equipment. Transition to roll-to-roll equipment follows the natural evolution of process development. Higher quality CIGS films can now be deposited with greater reproducibility, allowing optimization of subsequent coating processes. As a result, record efficiencies were achieved during Phase II for devices fabricated entirely using all roll-to-roll processes in large-area production-based equipment. The JV characteristic of the best device thus far, with an efficiency of 10.4%, is shown in Figure 1.23. Grid deposition and device characterization were conducted at IEC.

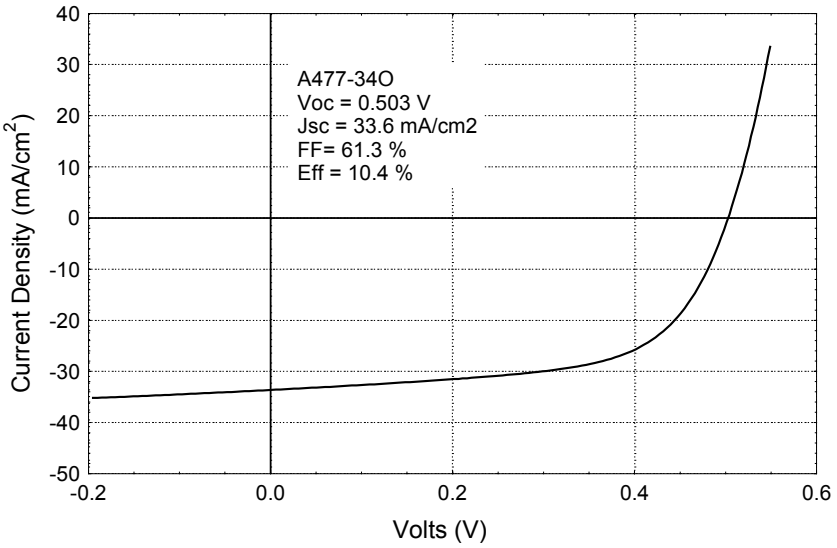

Figure 1. 23 JV characteristic of device formed completely at GSE in roll-to-roll processing on stainless steel.

1.5 Process Scaling and Repeatability

The objective of this task is to evaluate the reproducibility, stoichiometric uniformity, and thickness of the absorber layer over long (33 cm × 300 meter) runs and from run to run to determine and minimize variability. A large number of mechanical, process and control issues must be addressed to satisfy this objective, many of them complex. The effusion sources must provide a uniform, repeatable flux. A process parameter space must be identified that is relatively insensitive to variables that are difficult to control precisely. Finally, sensors and models are required to respond appropriately to dynamic system characteristics.

A near-term (2001) goal is to extend uniform quality CIGS coatings to a web length of nearly 1000 feet. During Phase II the maximum-coated web length was increased from 150 feet to nearly 500 feet while maintaining satisfactory composition along and across the web. Deposition lengths greater than 200 feet were routinely achieved without significant problems. The composition uniformity of one of the longest runs (P306) conducted thus far is shown in Fig. 1.24. Samples were extracted at a distance of two inches from the web edge. The specification limits established for Cu/(Ga+In) are 0.78 (LCL) and 0.93 (UCL).

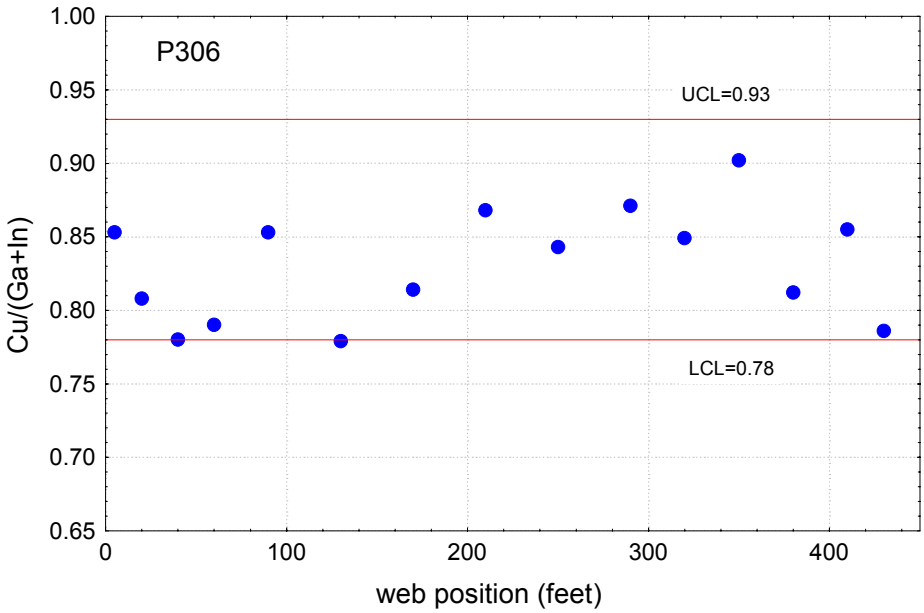

Figure 1. 24 CIGS composition along a 450-foot web.

Large-scale characterization of device yield was instituted for virtually all lots in Phase II. Sample coupons are extracted after all coating processes and test devices are fabricated and characterized. A histogram of device efficiency obtained from a representative lot is shown in Figure 1.25. All coatings on this lot were deposited at GSE in roll-to-roll production-based equipment. Devices were randomly selected from the 50-foot long section of stainless steel web. Median efficiency is over 8% with a tight distribution.

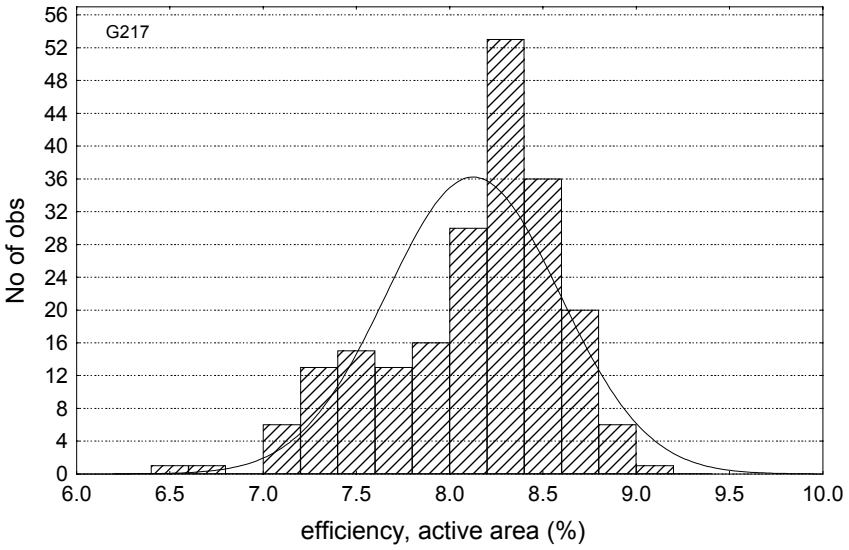

Figure 1. 25 Efficiency histogram for lot G217.

2.0 MONOLITHIC PROCESSES FOR INTEGRATION OF LARGE AREA PV

The objective of Task 2 is to develop low-loss scribe and interconnect processes for module formation. Our approach includes layer-specific, all-laser scribing methods, coupled with the development of ink-jet deposition of insulating material over scribes. The post-absorber interconnect, shown in Fig. 2.1 below, is formed using only two steps in the process sequence. In the first step the back contact and interconnect scribe are cut, and the back contact scribe is backfilled with insulating material in an ink-jet operation. After TCO deposition a second laser operation is used to cut the front contact scribe.

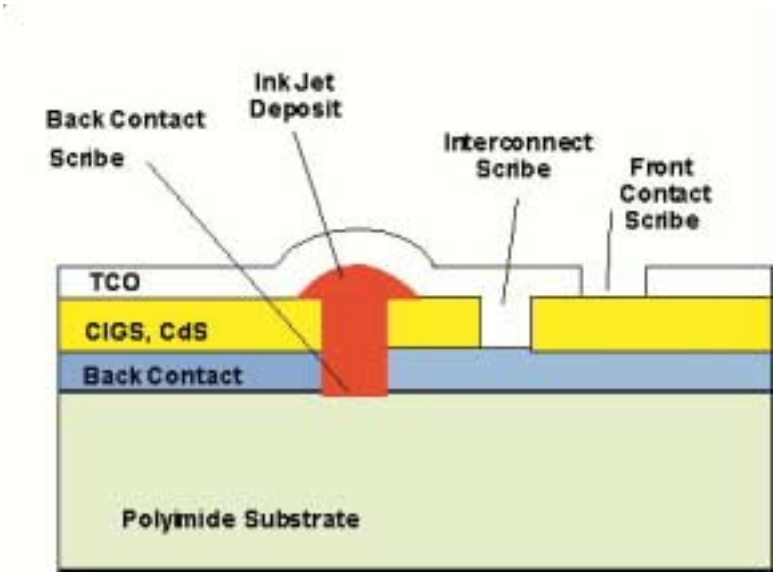

Figure 2. 1 The GSE post-absorber interconnect scheme

All laser processing is used because mechanical scribing is problematic with the flexible polyimide substrate and because mechanical scribing has several drawbacks in a high volume manufacturing operation. Selective cutting is crucial to the approach. The back contact must be scribed with minimal damage to the underlying substrate, and the interconnect scribe must leave the back (at least partially) intact. Damage to the absorber layer must be avoided when scribing the front contact.

2.1 Back Contact Scribes

Scribing conditions for laser processes were developed for the back contact scribe, "via" or interconnect scribe and the front contact scribe during Phase I. Process development for all three scribing operations was guided primarily by microstructural observations; only the back contact scribe had undergone electrical testing. Further improvements and validation of all three scribes has been accomplished in Phase II, including electrical testing of the interconnect scribe and the front contact scribe. Electrical tests have validated the functionality of the interconnect and front contact scribes and have allowed estimation of module losses.

Absent any shunt-induced loss, the back contact scribe electrical losses are governed by current leakage across the scribe. A typical distribution of resistance across back contact scribes is shown in Fig. 2.2. For reference, a 200Ω scribe resistance in the module pattern used for the data in Fig. 2.2 would represent about a 0.5% power loss for that segment. As indicated by the data in the figure, the loss expected due to back contact scribe leakage is negligible.

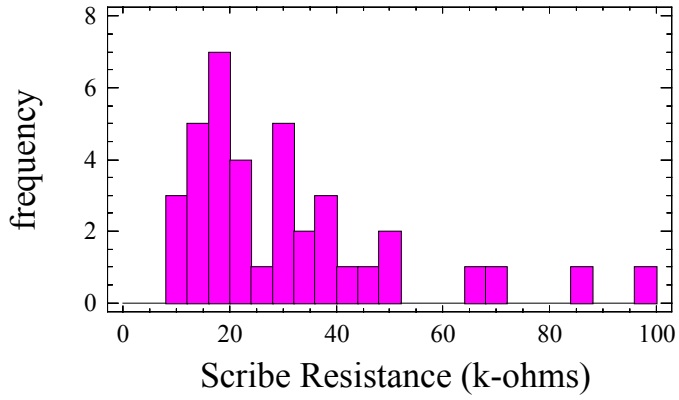

Figure 2. 2 A histogram showing the distribution of resistance across a typical set of back contact scribes.

2.2 Interconnect Scribes

Interconnect or "via" scribes have been optimized with microscopic evaluation and using interconnect test patterns. Interconnect test patterns, such as that shown in Fig. 2.3 were used to separate the resistance components due to the top contact and any possible influence of the ink-jet deposited insulator from the actual specific via resistivity.

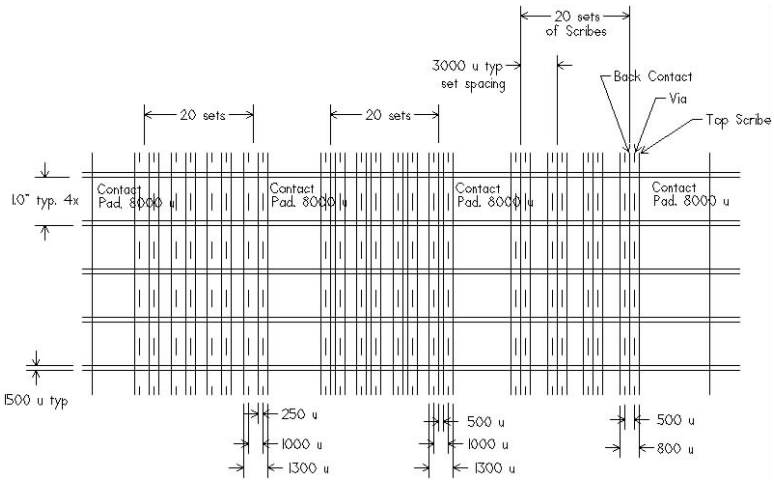

Figure 2. 3 The interconnect test pattern design utilized at GSE to isolate individual resistive components in the current collection path.

Initial evidence indicated that the resistance of the front contact might be increased locally where it goes over the ink-jet deposited insulator. Electron microscopy was used to look for step coverage problems, as discussed in the section explaining the ink-jet deposition. Further tests indicated that the effect of increased resistance near the interconnect was limited to modules and test patterns having a TCO with higher than normal sheet resistance.

An example of a via scribe is shown in Fig. 2.4. Regions where the back contact/substrate are exposed are apparent in the micrograph.

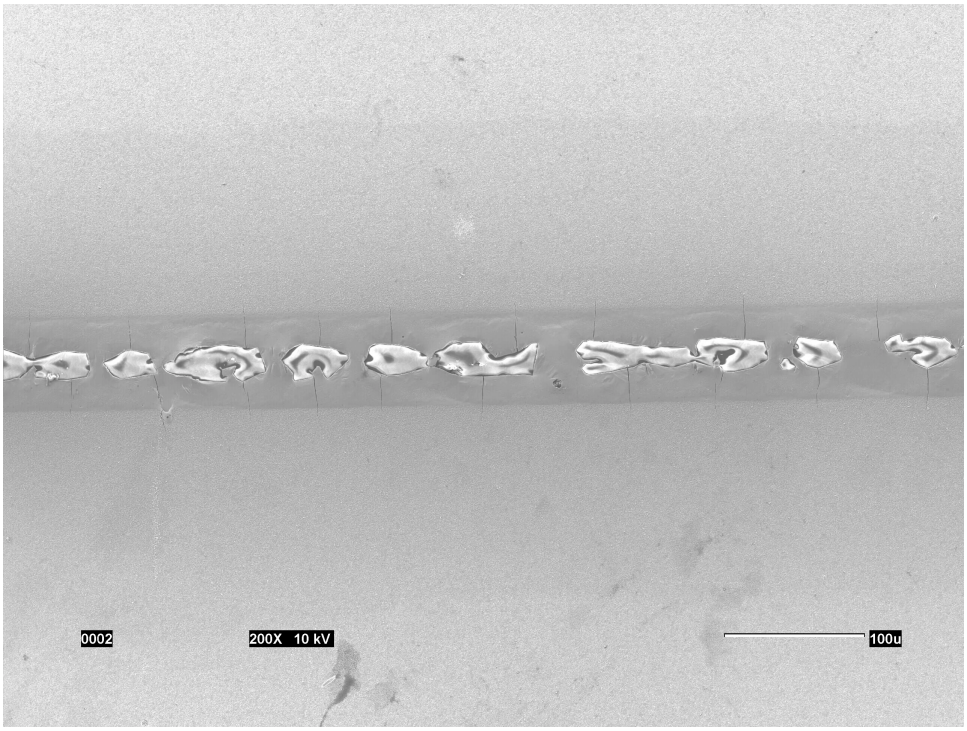

Figure 2. 4 SEM image of a laser process via scribe showing areas cut completely through the absorber layer.

Laser interconnect produced at GSE have specific resistivities as low as 0.3 ohm-cm. This corresponds to less than 2% power loss for an efficient module segment.

2.3 Front Contact Scribes

Definitive evidence validating the selective scribing for the front contact was obtained during Phase II. Microstructural and compositional data generated during Phase I verified the interruption of the TCO layer and removal of the elemental constituents of that layer. Even with microstructural and compositional data showing complete TCO removal, the possibility existed for shunting in the scribe area from the front to back contact, and shunting across the scribe between adjacent front contacts. Further tests were performed to validate the efficacy of the front contact scribe.

Electrical tests to determine the presence of shunting between adjacent segments across the scribe consisted of isolating small-area devices in a matrix pattern with the laser. The open-

circuit voltage of individual devices was then measured with and without optically masking all the surrounding cells. Incomplete front contact scribes or surface conductive layers within the scribe, causing pad-pad shunting, are revealed by a severely reduced V_{oc} for the device under test in the masked condition compared to the unmasked. As shown in Figure 2.5, the actual change in V_{oc} is small and appears to be due to random measurement error, probably reflecting positioning errors in the cell mask.

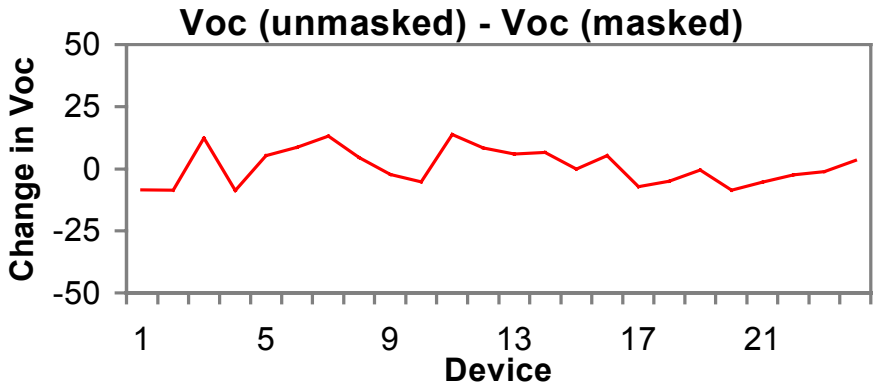

Figure 2. 5 Difference in Voc (in mV) for masked and unmasked conditions for cells isolated by the top contact using the selective laser scribing process.

Front contact scribes using the all laser process have been reproduced over multiple lots of material with good results. Tests indicate that the front contact scribing process is acceptable over a wide range of operating conditions, implying a robust process.

Predictably, the scribe width does vary with laser power (Fig. 2.6). Although good isolation across the front contact scribe has been obtained with very narrow scribes, repeatability is an issue. A front contact scribe 50 µm wide is employed to ensure process robustness. Factors such as scribe spacing and ink-jet line width are much stronger determinants of area loss when the scribe width is 50 µm.

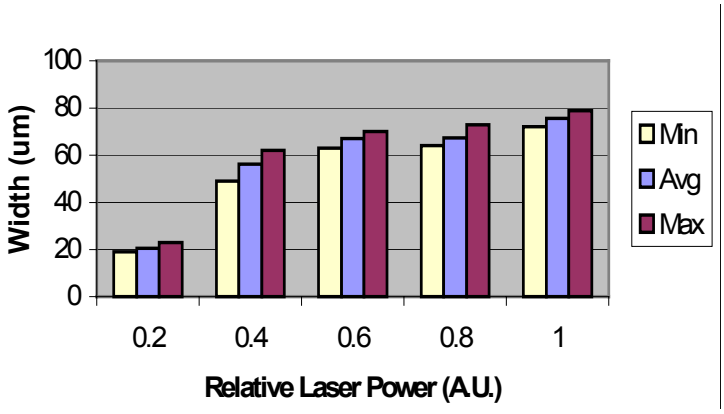

Figure 2. 6 Front contact scribe width versus laser power (relative units).

2.4 Ink Dispense Technology for Module Integration

Increased TCO resistivity over a line of ink-jet printed insulating material was observed at the start of ink evaluation trials. Incomplete step coverage as well as other mechanisms were considered. In Fig. 2.7 (A) a perspective view of ink-jet printed line from modules with a TCO front contact in place reveals furrows or wrinkles in the material caused by shrinkage in the polymeric adhesive upon drying. A number of microscopic examinations were made of the ITO adjacent and over the insulating material. Composition analysis was also employed to identify potential thinning (caused by shadowing or outgassing during ITO deposition) of the ITO on or immediately adjacent to the printed line. The results indicated that these effects were not responsible for the high series resistance.

Other adhesives subsequently investigated allowed thinner linewidths and improved uniformity. As a byproduct, the same adhesives exhibited less shrinkage or deformation upon drying, as shown in Fig. 2.7 (B). No significant problems were apparent when these inks were evaluated for TCO resistivity over the printed area. Although the source of the problem with the inks used early on was not fully determined, the issue was considered resolved and further investigation unwarranted.

A **B**

Figure 2. 7 Perspective views of the edge of an ink-jet printed insulating line showing fissures covered by TCO (A) and an insulating line made with an adhesive that avoids shrinkage, and formation of fissures (B).

At present, excessive area is sacrificed to the interconnect in order to improve process robustness. It is anticipated that after the excess scribe spacing is removed, the major limitation on total interconnect width will be the ink-jet printed insulating material over the back contact scribe. Minimizing interconnect area loss required further improvement in both the printed line width and in the printed line uniformity.

Accordingly, effort was directed toward improving the ink-jet printing characteristics. Many variations on dispense head pressure, dispense orifice size, adhesive type and viscosity and dispense tip-to-substrate distance were evaluated. Optimization of these operating parameters

resulted in improved linewidth and uniformity. In the best circumstances the linewidth obtained was 120 μm on a CIGS substrate (Fig 2.8).

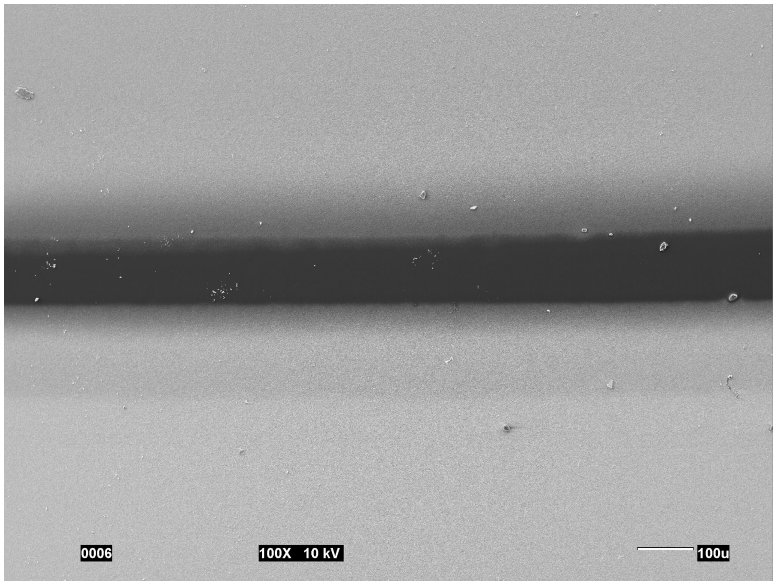

Figure 2. 8 Micrograph of a printed ink jet line on CIGS/CdS.

Another factor that can affect total interconnect width is the accuracy to which the scribe and ink-jet patterns can be maintained parallel and registered accurately. Maintaining parallel motion between laser and ink-jet operations has been accomplished to a high degree (Fig. 2.9). Registration accuracy and reproducibility has also been good, typically about 25 microns between operations on a given set of scribes.

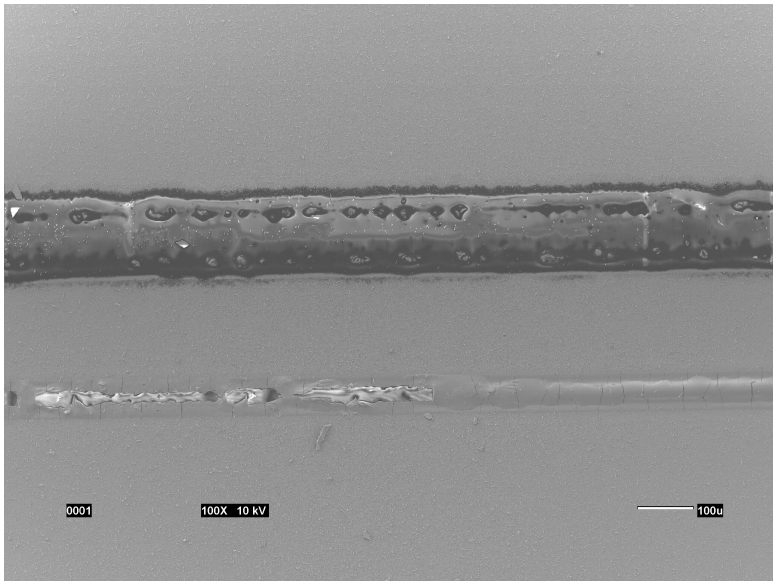

Figure 2. 9 SEM micrograph of an ink-jet deposited line (upper structure) over a back contact scribe (not visible) registered to the via scribe (lower structure).

All three scribing processes were combined with the ink-jet process for printing insulating material over the back contact scribe to form complete monolithic module interconnects. Figure 2.10 shows a completed module interconnect consisting of a front contact, "via" and back contact scribe (from top to bottom). Scribe spacing is intentionally quite large for diagnostic purposes. After process optimization is complete the scribe spacing will be reduced to minimize module area loss.

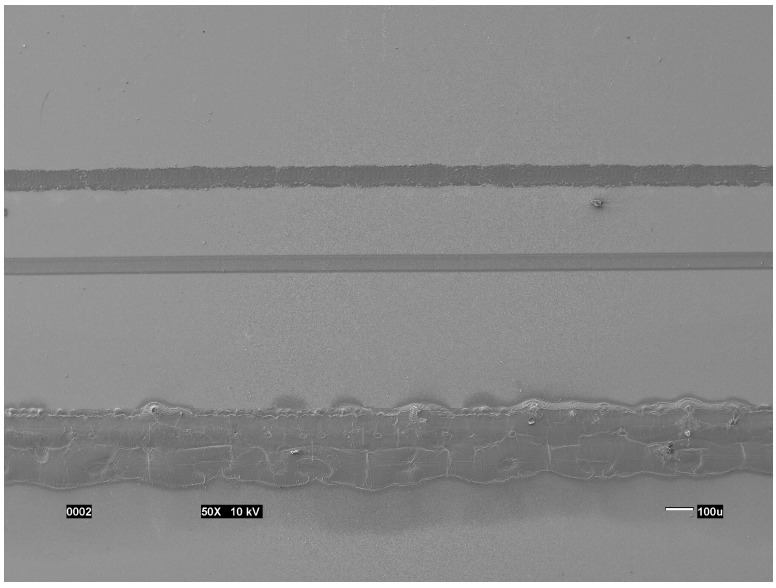

Figure 2. 10 Micrograph of all-laser scribing processes combined with the ink-jet printed insulator to make a functional module interconnect

Functional modules have resulted from the majority of lots completed with the optimized monolithic integration processes. Serial addition of voltage is realized, in most cases equal to that expected (the product of the average device V_{oc} and the number of module segments). In some cases, some shunting was observed that reduced module V_{oc} moderately. The shunting in these cases appeared to be associated with an incomplete "edge termination" scribe around the periphery of the module used to define the aperture area. Improvements in CIGS uniformity and device efficiency are required to allow further optimization of the monolithic integration processes.

2.5 Conclusions and Future Work

Substantial progress has been made in the development of all-laser processes for monolithic integration. All laser scribes have been demonstrated and optimized to minimize electrical losses. Further work will be done to characterize the interconnect resistivity over wider ranges of laser power.

Ink-jet deposition of insulating material over the back contact scribe has also been successfully demonstrated at fairly narrow linewidths. Modifications to allow still finer linewidth and better

control will be implemented, including modifications to the ink-jet equipment and dispense tips. Software and machine vision improvements will be incorporated into the motion control of the scribing station that will more easily enable precise control over line spacing. Module loss analysis will be used to continually identify the largest potential areas of improvement.

3.0 ENCAPSULATION DEVELOPMENT AND RELIABILITY TESTING

The overall objectives of this task are to develop a viable, high-quality, rapid-throughput encapsulation and finishing methodology to produce both flexible and rigid-mounted PV products. Primary efforts within this task have been toward development of flexible and semi-flexible backed products based on a structure of Tefzel/EVA/Thin module/EVA/Selected Backing Material (depends on product line).

During the second year of this subcontract, the focus within this task has been primarily on:

- Refocus of module design to meet the requirements of a PV module utilizing flexible metal substrate in addition to the polymer substrates, both used by GSE.
- Further demonstrations of new module designs (unlaminated, flexible, semi-flexible, and rigid).
- Screen Testing and Pre-Certification of various module designs.

The primary accomplishments within the new product development and demonstration area at GSE include:

- Development of unlaminated submodules, with a strategic business partner, on a rigid substrate for use as a roof shingle
- Development of modules that utilize a reinforced nylon backing that provide support for two GSE product lines with attributes of lightweight, durability, and portability. No junction box is utilized in this design.
- Development of modules that utilize a semi-rigid, thin aluminum backing for added strength in the field and for a standard UL rate-able product line. Designs have been submitted to UL and a contract for UL testing is in place.
- Procurement and placement of critical product certification equipment at the GSE Tucson facility to accelerating the required testing.
- Demonstration of products in selected market sectors for early feedback from customers.

3.1 GSE Product Description

GSE has developed five initial product lines envisioned to meet the needs of the initial markets identified. The goals of this NREL subcontract have allowed focused efforts to be applied towards developing and demonstrating first generation product designs. Certification of products will become a primary focus for GSE in the future. One of the primary competitive advantages of the GSE technology is the ability to make whatever size and design of product is necessary to meet market needs without complex or expensive re-tooling. Furthermore, it is clear from the following that the ability to attach the flexible GSE substrate to a variety of module backings (including curved, flexible, and non-flexible materials) is much more feasible than for most other PV technologies.

1. Unlaminated **Submodules** for product lamination and finishing via strategic, specialty partners (Fig. 3.1)

2. **Portable Power Pack's™;** foldable, flexible modules with reinforced nylon backing (Fig. 3.2)
3. **Power Flex™,** foldable, flexible power modules with reinforced nylon backing (Fig. 3.3)
4. **Power Flex™ Semi-Flexible;** power modules with aluminum backing, mainstream framing, to be UL listed (Fig. 3.4)
5. **Transportable AC Systems (TACS);** PV-Battery system with generator backup (Fig. 3.5)

Unlaminated Submodules

GSE plans to provide unencapsulated submodules to strategic partners already having capabilities to incorporate these modules into PV products familiar to that partner. The first of many such products is a roofing shingle on a rigid substrate. Several prototypes have been successfully accomplished and further optimizations will continue. Figure 3.1 shows an example of this type of roofing shingle product. Lamination in this case utilizes standard EVA encapsulant and a durable glass cover sheet.

Figure 3. 1 Photograph of roofing shingle incorporating GSE's photovoltaic submodules.

Portable Power Pack for Communications

GLOBAL SOLAR'S **Portable Power Pack™** photovoltaic modules offer a completely new solution for reliable and portable power. When folded, the module's lightweight and compact size make it the most transportable solar module available. When unfolded, the module can be easily mounted in any position on flat or curved surfaces using its built-in mounting holes (Fig. 3.2). No junction box in the module is required, and the leads are sufficiently stress relieved. The **Portable Power Pack™** modules provide a cleaner, economic and lightweight energy source for hikers, campers, and boaters, with direct application to police and military operations. Portable computer and cell phone users can benefit as well. These small arrays can be stowed in survival kits, and can be used in remote applications where access to electric power is otherwise impossible.

The module's design is simple to use and maintenance free. Modules are easily folded into compact size for quick transport and convenient storage. Furthermore, the module's flexibility, light weight, and built-in grommets allows for hanging, mounting, or laying in any position on any surface shape with no heavy support structure required.

A particular application, developed for the U.S. Marines this last year, but applicable throughout the Military, incorporates a miniature battery charge controller for use with small lead-acid batteries or Nickel-Metal-Hydride batteries tied together with the portable power pack module. Such a product can recharge a 7A-hr battery in a single day providing self-sustained power for radios that is quiet and portable.

Figure 3. 2 Photograph of GSE's Portable Power Pack™.

GSE's Power Flex™ Products

GLOBAL SOLAR'S **Power Flex™** photovoltaic (PV) modules (Fig. 3.4) offer a completely new solution for reliable solar energy. Weighing approximately 90% less than conventional PV modules and with a flexible physical form replacing fragile glass, the **Power Flex™** modules offer extensive usage, handling, installation and shipping benefits. These are key advantages for cost-effective turnkey PV systems. Another cost and weight minimization advancement for this product comes from avoiding the use of a junction box.

The **Power Flex™** modules are a lightweight, flexible and durable solar energy source for Power Tents, Large, Lightweight and Portable Arrays, PV Power Systems, Building-Integrated PV, Commercial and Residential Systems, and all applications requiring clean fuel-free power. The module's design is simple to use and maintenance free. It is fully encapsulated and is damage tolerant when mishandled, hailed upon or hit by debris. As a result, it requires low maintenance and thus, provides a low operating cost.

A more rigid version of a **Power Flex™** module is shown in Figure 3.3. This **Power Flex™ Semi-Flexible** module is intended to be UL listed in the near future. It is expected to enhance the flexible **Power Flex™** market since it can address those markets that require a stiffened backing, either with or without a mainstream frame. A mainstream junction box is used for the majority of these **Semi-Flexible Power Flex™** modules.

Figure 3. 3 Photograph of a PV array utilizing the GSE Power Flex™ Semi-Flexible Module

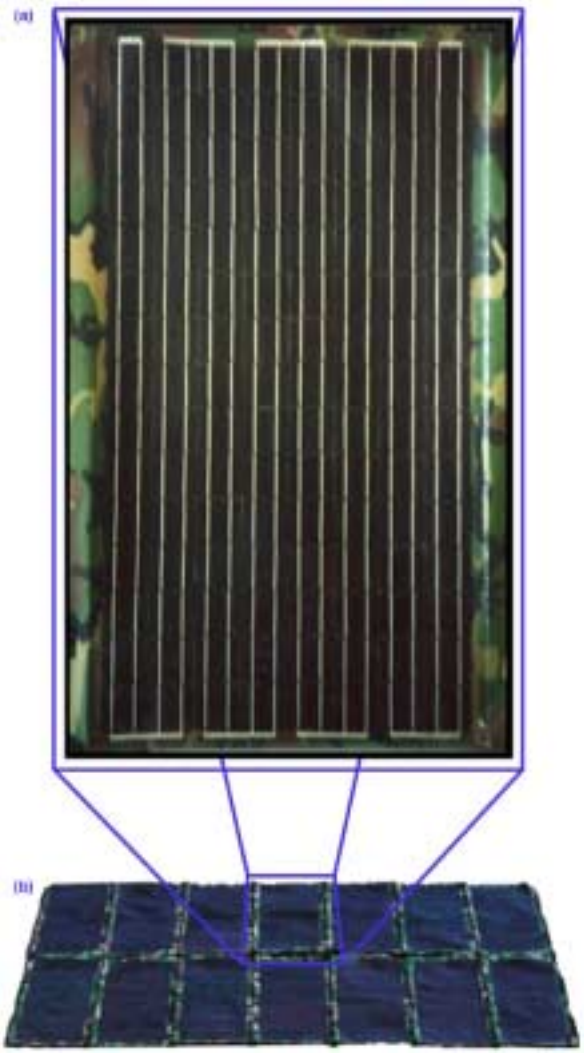

Figure 3. 4 Photograph of the (a) GSE Flexible CIGS "Power Flex™" Module and (b) "Power Flex™" Flexible Array.

Transportable AC System (TACS)

GLOBAL SOLAR'S **Transportable AC Systems (TACS)** provide the convenience of reliable electricity in nearly any location or situation. Each system is supplied with clean, silent power from a lightweight, flexible and durable solar array fabricated from **Power Flex™** modules. Excess power from the solar array is stored in a battery bank for nighttime or cloudy day use, and additional or backup power is supplied by a generator connected to the system's control unit (Fig. 3.5).

The solar array of each **TACS** utilizes GLOBAL SOLAR'S **Power Flex™** solar modules. The fully integrated TACS readily supplies 120VAC power with standard plug-ins while offering several other benefits, including minimizing environmental impacts, reduced fuel cost, transportation, and storage and associated logistics, predetermined generator runtime to mitigate

generator noise, reduced generator maintenance, prevention of "wet stacking" by the ability to run generators at optimal loads, increased dynamic power-producing range by combining outputs of stored energy and backup sources (PV and genset), and transportability for use in any location. Furthermore, the system can provide much cleaner power to sensitive electronic components than a traditional genset, particularly during load. These modules are designed for rapid deployment and stowage, and can be folded and stowed in a 62" × 30" × 25" container for easy transport.

Figure 3. 3 Photograph of TACS Power Storage and Backup Generator System.

A similar, but alternative application for GSE **Power Flex™** modules has been the development of a portable power system to be attached to General Personnel TEMPER tent for the military as shown in Figure 3.6. The TEMPER tent is one of the most heavily used structures in today's military, providing a rapidly-deployed, versatile habitat for use as barracks, offices, communication centers, medical centers, commissaries, and storage. These structures are deployed by assembling a metallic frame under an unfolded canvas structure. The lightweight, durable nature of the module arrays is key to success in this application.

Figure 3. 4 Photograph of TACS Power Storage and Backup Generator System.

3.2 High Speed Lamination

The objective of this subtask is to design, fabricate, install, and test lamination equipment capable of low-cost lamination of solar panels that meet initial throughput, economic, and market needs of GSE. Due to the early efforts and experience with prototype equipment, equipment to meet the initial lamination goal rate of ~1ft^2 per minute has been standardized.

3.3 Lamination of Flexible Substrate to Low Cost Rigid or Semi-Flexible Backing

During this program, the following materials have been evaluated in order to make the decision to focus on the appropriate semi-flexible backing material.

Semi-Flexible

- Aluminum,
- Reinforced epoxy sheets utilized in PC boards
- Galvanized steel,
- Polypropylene,

Rigid

- Shingle slate
- Glass

Reinforced epoxy sheets utilized in PC board manufacturing were evaluated as a backing material. The associated mechanical and adhesion properties are desirable. Questions arose related to the ability of the material to withstand UV after years in the field. UV stability concerns need to be addressed through further stress testing. Aluminum was therefore chosen as a backing material since it seems to have all the advantages and none of the unproven characteristics of reinforced epoxy. Aluminum is electrically conductive, so as a potential second-generation design, the glass-reinforced epoxy backing material may still be of value. Galvanized steel may provide the lowest cost option in the longer term.

The effort on rigid substrates has resulted in product demonstrations on roof shingles as described in "GSE Product Descriptions". Glass is only utilized at present as a comparative industry standard for stress and certification testing.

3.4 Power Lead and Buss Attachment

The objective of this subtask is to design, demonstrate, and incorporate parts, materials, and procedures for the range of steps in solar module fabrication from buss bar application to power lead attachment in order to meet initial throughput, economic, and market needs of GSE. Each of the products described in the "GSE Product Description" section are now relatively well defined in the Power lead and buss attachment areas.

The reinforced Nylon backed modules (**Portable Power Pack™** and **Power Flex™)** utilize stitched stress relief areas and no junction boxes on the module. Incorporation of a bypass diode or a blocking diode, as desired, into the module structure rather than in the cable is being evaluated. A defined wire specification and appropriate stress relief (in the case of the flexibles) results in easily passing the UL power lead Strain Relief Test.

Buss Bars

The primary requirement for a buss bar system is to make a low resistance contact to the electrodes on the end cells of a module and to retain those properties over stresses representative of the environment of use.

Buss bar tape and conductive inks were selected for these product designs. On some of the buss bars, these selective conductive pastes were applied to evaluate improved contact reliability. Test dummies were fabricated with the goal of monitoring resistance changes during stressing, and initial stresses were accomplished. The contact resistance was determined at various points in the test including:

- Before lamination
- After lamination
- Before and after mechanical rolling of the dummy over a 3" diameter pipe
- After thermal stressing at 90C for 1 hour
- After thermal stressing at 90C for 24 hours

Table 3.1 shows the calculated increased power losses (I^2R) due to resistance increase of buss bar contacts for four different chosen materials/configurations. It is assumed that a reasonable

allowable power loss threshold for modules is 0.5%. The absolute error associated with these values is ~ ± 0.01%.

Table 3. 1 Power losses calculated from resistance change measurements for several conductive adhesives used for buss bar attachment.

Condition	After Lamination	Before Mechanical Stressing	After Mechanical Stressing	After 1 Hour at 90C	After 24 Hours at 90C
No Paste	0 (Baseline)	0.09%	0.10%	0.18%	0.23%
Paste B	0 (Baseline)	0.014%	0.033%	0.024%	0.10%
Paste C	0 (Baseline)	0.14%	0.19%	0.26%	0.66%

The conclusions of this test are that:

1) For initial, short term stresses, for No Paste and for Paste A, there appears to be no real issue with increases in power loss due to resistance increase of the buss bars or contacts to TCO layer.
2) There are choices of paste that make the effect worse.
3) More stress testing will need to be accomplished.

To ensure that the selected buss bar system remains stable during its life in the field, well designed thermal exposure, humidity exposure, and thermal cycling tests are intended to be accomplished utilizing not only the best choices from this test but with other selections as well.

3.5 Module Performance and Reliability Testing

The goal of this subtask is to develop and utilize appropriate tests and equipment for proper screening and evaluation of module efficiency and reliability. Passing UL tests is paramount to success in the PV roofing and building market, so much focus has been toward a module design that will become UL rated.

The team has incorporated Module Performance and Reliability Testing equipment at the GSE Tucson facility. The in-house capabilities now include:

- Pulse-Simulator for large area module testing with upgraded IV testing hardware
- New 6-in. diameter area continuous Xenon source for accurate cell testing
- Thermal cycling, humidity-freeze cycling, and humidity soak chamber
- Temperature soak oven
- Hi-Pot tester
- Cut test
- Static loading test

In addition, IEEE 1262 are scheduled to be accomplished at ASU with a primary goal of assuring and certifying the reliability of a high performance product. A few of the areas of concern with regard to flexibles and semi-flexibles with Tefzel top layer are discussed:

As noted above, without a junction box the stresses applied to the leads were a concern. After incorporation of simple and appropriate stress relievers, the modules passed the lead loading tests with ease.

With flexible modules, the 50lb/ft^2 Static Loading Test was a concern.

1) The **Power Flex™** module backed with a flexible rip stop passed the static loading test at GSE after incorporating lightweight reinforcements around the border periphery, and
2) the **Power Flex™ Semi-Flexible** backed with light gauge aluminum easily passed the static loading test at GSE.

During the next phases of this subcontract, the focus within this subtask will be primarily on further demonstration, stress testing, and certification of aluminum backed **Power Flex™ Semi-Flexible** modules and of **Power Flex™** modules.

Summary and Future Efforts

Future efforts within this task of this subcontract include the following:

- a multitude of product stressing and certification tests, including UL, IEEE, and others
- further product design enhancements of flexible, semi-flexible, and rigid module products for stressing and certification testing

With an initial product line identified and substantially defined, stress testing and certification testing are the critical items of focus as we move forward with a state-of-the art product line. Considerable effort will be required to effectively accomplish these product development and certification goals.

Summary

During the second year of effort under this subcontract, a number of significant advancements were made. Improvements to the effusion source design and operation have been demonstrated. At present, the robust effusion sources are capable of depositing high quality coatings over large areas. Significant challenges still exist for increasing the source capacity to enable even longer depositions and improving the control of effusion rate during production runs.

Another significant accomplishment that occurred during Phase II was the demonstration of a 11.5% efficient device from CIGS deposited on stainless steel web. That milestone was the result of a deeper understanding of the CIGS deposition process as practiced by GSE. In addition, process improvement tests validated the beneficial effects of Na doping which was subsequently implemented in the production equipment. The compatibility of GSE processes for CdS and the TCO depositions was continuously verified as improvements in the absorber deposition process were made.

Substantial improvement of the monolithic integration of PV cells on polyimide substrate has been made. Most aspects of the back contact, via, and front contact scribes have been rigorously verified by electrical and microscopic techniques. The ink dispense technology, an integral part of the interconnect scheme, has demonstrated continuous ink lines less than 200 μm wide, with exceptional reproducibility.

Numerous accomplishments within the new product development and demonstration area at GSE have been achieved. Unlaminated submodules on a rigid substrate for use as a roof shingle have been developed with a strategic business partner. Modules that utilize a reinforced nylon backing that provide support for two GSE product lines with attributes of lightweight, durability, and portability have also been developed. Modules that utilize a semi-rigid, thin aluminum backing for added strength in the field and for a standard UL rate-able product line have been demonstrated. The semi-rigid module designs have been submitted to UL and a contract for UL testing is in place. Critical product certification equipment has been procured and validated at the GSE Tucson facility to accelerate the required testing. Products have been demonstrated in selected market sectors for early feedback from customers

Future Plans

Moving into Phase III, even greater emphasis will be placed on improving the yield, reproducibility, and throughput of the CIGS deposition step. The average test device efficiency goal is 9.0% by the end of Phase III and a well-defined plan for reaching that goal is being implemented. More tolerant regions of the CIGS deposition parameter space will be sought.

Regarding monolithic integration, further work will be done to characterize the interconnect resistivity over wider ranges of laser power. Modifications to allow still finer linewidth and better control will be implemented, including modifications to the ink-jet equipment and dispense tips. Software and machine vision improvements will be incorporated into the motion control of the scribing station that will more easily enable precise control over line spacing.

Module loss analysis will be used to continually identify the largest potential areas of improvement.

Future efforts within this task of this subcontract include the following:

- a multitude of product stressing and certification tests, including UL, IEEE, and others
- further product design enhancements of flexible, semi-flexible, and rigid module products for stressing and certification testing.

Acknowledgements

Global Solar Energy wishes to acknowledge the contributions of the following people and organizations:

The Global Solar Team:
S. Albright, M.E. Beck, R. Butcher, J. Britt, J. Chaney, J. Fogleboch, S. Kennedy, R. Huntington, D. Magni, D. Mason, J. Muha, D. Shah, E. Sheehan, R. Wendt, and S. Wiedeman.

Other contributors:
F. Hasoon, R. Noufi, E. Eser, W. Shafarman, B. Birkmire, A. Rockett, and A. Swartzlander

IEC
NREL

This work has been supported in part by NREL subcontract ZAK-8-17619-04.

REPORT DOCUMENTATION PAGE

Form Approved
OMB NO. 0704-0188

1. AGENCY USE ONLY (Leave blank)	2. REPORT DATE	3. REPORT TYPE AND DATES COVERED
	November 2000	Phase II Technical Report

4. TITLE AND SUBTITLE
Process Development for CIGS-Based Thin-Film Photovoltaic Modules;
Phase II Technical Report

5. FUNDING NUMBERS
C: ZAK-8-17619-04
TA: PVP15001

6. AUTHOR(S)
J. Britt, S. Wiedeman, and S. Albright

7. PERFORMING ORGANIZATION NAME(S) AND ADDRESS(ES)
Global Solar Energy, L.L.C.
5575 South Houghton Road
Tucson, AZ 85747

8. PERFORMING ORGANIZATION REPORT NUMBER

9. SPONSORING/MONITORING AGENCY NAME(S) AND ADDRESS(ES)
National Renewable Energy Laboratory
1617 Cole Blvd.
Golden, CO 80401-3393

10. SPONSORING/MONITORING AGENCY REPORT NUMBER
NREL/SR-520-29227

11. SUPPLEMENTARY NOTES
NREL Technical Monitor: H.S. Ullal

12a. DISTRIBUTION/AVAILABILITY STATEMENT
National Technical Information Service
U.S. Department of Commerce
5285 Port Royal Road
Springfield, VA 22161

12b. DISTRIBUTION CODE

13. ABSTRACT *(Maximum 200 words)*

As a technology partner with NREL, Global Solar Energy (GSE) has initiated an extensive and systematic plan to accelerate the commercialization of thin-film photovoltaics (PV) based on copper indium gallium diselenide (CIGS). The distinguishing feature of the GSE manufacturing process is the exclusive use of lightweight, flexible substrates. GSE has developed the technology to fabricate CIGS photovoltaics on both stainless-steel and polymer substrates. CIGS deposited on flexible substrates can be fabricated into either flexible or rigid modules. Low-cost, rigid PV panels for remote power, bulk/utility, telecommunication, and rooftop applications have been produced by affixing the flexible substrate to an inexpensive rigid panel by lamination or adhesive.

Stainless-steel-based PV modules are fabricated by a novel interconnect method that avoids the use of wires or foils and soldered connections. In the case of polymer-based PV modules, the continuous roll is not sectioned into individual panels until the module buss and power leads are attached. Roll-to-roll vacuum deposition has several advantages that translate directly to reduced capital costs, greater productivity, improved yield, greater reliability, lower maintenance, and a larger volume of PV material. In combination with roll-to-roll processing, GSE has developed evaporation deposition operations that enable low-cost and high-efficiency CIGS modules. The CIGS deposition process relies heavily on effusion source technology developed at GSE, and solving numerous problems was an integral part of the source development effort. Cell interconnection for thin-film CIGS modules on a polyimide substrate presents a considerable challenge.

14. SUBJECT TERMS
photovoltaics ; copper, indium gallium diselenide (CIGS) ; lightweight and flexible substrates ; stainless-steel substrates ; polymer substrates ; thin film ; rigid PV panels ; roll-to-roll processing ; evaporation deposition ; CIGS modules

15. NUMBER OF PAGES

16. PRICE CODE

17. SECURITY CLASSIFICATION OF REPORT	18. SECURITY CLASSIFICATION OF THIS PAGE	19. SECURITY CLASSIFICATION OF ABSTRACT	20. LIMITATION OF ABSTRACT
Unclassified	Unclassified	Unclassified	UL